4-2010

MODEL-BASED CONTROL WITH STOCHASTIC SIMULATORS: BUILDING PROCESS DESIGN AND CONTROL SOFTWARE FOR CATALYTICALLY ENHANCED MICROSYSTEMS

Matthew T. Curnan
University of Pennsylvania

Arjun Gopalratnam
University of Pennsylvania

Charles G. Slominski
University of Pennsylvania

Eric Wang
University of Pennsylvania

MODEL-BASED CONTROL WITH STOCHASTIC SIMULATORS: BUILDING PROCESS DESIGN AND CONTROL SOFTWARE FOR CATALYTICALLY ENHANCED MICROSYSTEMS

Abstract
The production, characteristics, dynamics, and economics of microreactors were studied in this report. Overall it was found that the best microfabrication techniques for small scale processes were laser ablation, the LIGA process, soft lithography, and anisotropic wet chemical etching, roughly in ascending order of effectiveness. One of the few viable bonding techniques was found to be diffusion bonding followed by microlamination, whereas many coating methods -- such as solgel coating, modified anodic oxidation, and electrophoretic deposition -- were effective in μTAS integration.

The high surface area to volume ratio of microreactors enables precise control of the temperature of the reactor along its axial dimension. Taking advantage of this feature in the design of microreactors leads to better control of complex reaction networks and generates more valuable effluent streams. A model predictive controller was implemented for the common, archetypical reaction network involving the hydrogenation and dehydrogenation of cyclohexene with various control objectives. It was found that the highest rate of production of benzene and cyclohexane occurred at 600 K while the most pure stream of benzene occurred at 200 K. Model predictive control was found to be highly resistant to the inherent stochasticity of small scale processes.

The market for a software-based controller for microreactors was surveyed and found to still be in the early stages of development. A profitability analysis was conducted for a start-up company using microreactors to make cyclohexane. A price of $18,000 for the product was found to be a reasonable selling price yet allowed the start-up to remain profitable.

Department of Chemical & Biomolecular Engineering

Senior Design Reports

University of Pennsylvania 2010

Model-Based Control with Stochastic Simulators: Building Process Design and Control Software for Catalytically Enhanced Microsystems

Matthew T. Curnan
University of Pennsylvania

Arjun Gopalratnam
University of Pennsylvania

Charles G. Slominski
University of Pennsylvania

Eric Wang
University of Pennsylvania

Model-Based Control with Stochastic Simulators: Building Process Design and Control Software for Catalytically Enhanced Microsystems

Chemical and Biomolecular Engineering 459
Professor Leonard A. Fabiano
April 27, 2010

Matthew T. Curnan
Arjun Gopalratnam
Charles G. Slominski
Eric Wang
Department of Chemical and Biomolecular Engineering
University of Pennsylvania

Project Advisor: Dr. Talid R. Sinno
Project Recommended By: Dr. Talid R. Sinno, University of Pennsylvania

April 27, 2010

Department of Chemical and Biomolecular Engineering
School of Engineering and Applied Science
University of Pennsylvania
220 S. 34th Street
Philadelphia, PA 19104

Dear Drs. Talid Sinno and Warren Seider, and Professor Leonard Fabiano,

Enclosed in this book is the final copy of our Senior Design Report on Model-Based Control with Stochastic Simulators: Building Process Design and Control Software for Catalytically Enhanced Microsystems. A software product consisting of a model predictive controller for use with stochastic processes was developed using kinetic Monte Carlo simulations to model chemical reactions carried out in a microreactor. The controller optimizes processes for a range of control goals and is capable of handling stochasticity inherent in reactions carried out in microreactors. The capability of the controller was tested through simulations of cyclohexene hydrogenation and dehydrogenation.

The current marketplace for a microreactor controller was found to be limited since microreactors have not yet been widely accepted in industry. A profitability analysis was performed to determine the feasibility and price of selling a microreactor controller to a start-up company producing benzene through the dehydrogenation of cyclohexene.

Sincerely,

Matthew T. Curnan Arjun Gopalratnam

Charles G. Slominski Eric Wang

Table of Contents

Abstract

The production, characteristics, dynamics, and economics of microreactors were studied in this report. Overall it was found that the best microfabrication techniques for small scale processes were laser ablation, the LIGA process, soft lithography, and anisotropic wet chemical etching, roughly in ascending order of effectiveness. One of the few viable bonding techniques was found to be diffusion bonding followed by microlamination, whereas many coating methods -- such as solgel coating, modified anodic oxidation, and electrophoretic deposition -- were effective in μTAS integration.

The high surface area to volume ratio of microreactors enables precise control of the temperature of the reactor along its axial dimension. Taking advantage of this feature in the design of microreactors leads to better control of complex reaction networks and generates more valuable effluent streams. A model predictive controller was implemented for the common, archetypical reaction network involving the hydrogenation and dehydrogenation of cyclohexene with various control objectives. It was found that the highest rate of production of benzene and cyclohexane occurred at 600 K while the most pure stream of benzene occurred at 200 K. Model predictive control was found to be highly resistant to the inherent stochasticity of small scale processes.

The market for a software-based controller for microreactors was surveyed and found to still be in the early stages of development. A profitability analysis was conducted for a start-up company using microreactors to make cyclohexane. A price of $18,000 for the product was found to be a reasonable selling price yet allowed the start-up to remain profitable.

1 Introduction to Microreactors

1.1 Definition and Characteristics of Microreactors

In the context of chemical microsystems, microreactors can generally be defined as miniature reaction systems operating from the nanometer to the sub-millimeter scale that are constructed through the methods and devices implemented in micro- and nanofabrication (Ehrfeld 2000). Traditionally these reactors were small, tubular, and used almost exclusively to test the performance of catalysts; however, recent improvements in the microfabrication of sensors and actuators on the same scale has allowed for their integration with microreactors to form micro-total-analysis-systems (μTAS). These systems are comprised of individual components – such as heat exchangers, mixers, and separators – that are known as *elements*. Upon integrating these elements into a single system via a continuously flowing fluid stream, each of them constitutes a fundamental structure or *unit* of the microsystem. By virtue of this construction, microreactor units are conducive to being linked in series to accomplish the tasks typically undertaken by macroscale reactors (Jensen 2001). Through this design project, microreactors will be studied in *reaction* – rather than *analysis* – systems. In the latter case, devices such as pulse microreactor-chromatographs are used to gather chemical data not directly involved in the optimization of an industrial process; a prime example of this is the acquisition of rate constants and energies of activation of the isomerization reactions of xylene over a zeolite catalyst (Li 1992). In contrast, reaction systems aim to find the optimal conditions at which a process should be run (Ehrfeld 2000), such as the control of cyclohexene hydrogenation and dehydrogenation to maximize the final concentration of either benzene or cyclohexane products (Nassar 2006).

1.2 Advantages and Considerations in Using Microreactors

In order to more fully appreciate the characteristic differences between typical macroscale reactors and microreactors, the differences themselves should be thought of as either property or production oriented. The differences in chemical properties largely allow microreactors to conduct reactions at more extreme conditions and thus achieve higher yields; specifically, the properties that enable this are:

- Heat Transfer Properties: In microreactors and the microfluidic channels leading to them, heat and mass transfer properties – such as heat transfer coefficients (h), hydraulic diameter (D_h), and Reynolds Number (Re) – are largely improved. This augmentation results from the high surface-to-volume ratio of microfluidic channels themselves, which is equivalent to their low values of D_h. For instance, the surface-volume ration of a 1.5 mL microreactor is 200 as compared to 0.6 for a 1 m^3 reactor. Considering that h is inversely proportional to D_h, heat transfer must increase with decreasing channel diameter. In addition, Re is directly related to D_h, meaning that outside of extreme cases, convection can almost always be modeled assuming laminar fluid flow holds (Incropera 2007).
    - For gaseous systems, continuum heat transfer equations are invalidated when D_h is on the same order of magnitude as or is less than the mean free path of the reacted gas.
    - In liquid reactions, approximations of velocity distributions and pressure drops of the fluid flow over the channels are invalidated when $D_h < 1$ μm.

- Pressure Drop: Due to the inverse relationship between the microchannel aspect ratio and the pressure drop (ΔP) in packed bed microreactors, higher, more dangerous pressure drops must be counteracted by decreasing channel length. In order to do this, cross-sectional channel area (A_c) must be maximized, which can be accomplished by splitting fluid flow over several channels and maintaining a high surface-to-volume ratio (Jensen 2001).

- Mass Transfer Properties: In packed bed reactors, the increase in surface-to-volume ratio of smaller catalyst pellets – which can be used here without raising ΔP unreasonably – has a similar effect on mass transfer. As an example of this, the cyclohexene hydrogenation reaction spread over multiple channels has a mass transfer coefficient of approximately 5-15 s^{-1}, significantly higher than that of standard reactors (0.01-0.08 s^{-1}). Therefore, mass transfer-limited processes can occur in microreactors while maintaining high productivity (Jensen 2001).
- Thermal Response Times: The thinness of the interior walls of the microchannels – which provides low thermal mass and strong thermal contact with the catalysts

lining them – have quick open-loop thermal response times (~10 milliseconds). This property is critical in temperature control applications, and considering that this response time is not limiting in achieving hydrogen flux, hydrogenation and dehydrogenation reactions can be carried out effectively (Jensen 2001).

- The Laminar Flow Regime: As mentioned before, laminar flow describes the flow in microchannels due to favorable heat transfer properties such as larger values of h (1,500-20,000 W/m^{2}K) and small values of D_h (Incropera 2007). As a result, uniform, nearly ideal temperature conditions can be applied over microreactors in very exothermic reactions, avoiding problems such as hot spots, dead zones, and explosive conditions that limit conventional reactors (Rawlings 2002).

- Reaction Pathways: On the macroscopic level, certain reaction pathways once considered too difficult to pursue in appreciable yields will now become more feasible due to the increase in heat transfer (Jensen 2001).

Microreactors differ from their macroscale counterparts in production-oriented and physical ways as well, leading to other distinctions between the two:

- Thinness of Channel Walls: As mentioned previously, volatile reactions such as oxidation, partial oxidation, and highly exothermic reactions are easier to run in microreactors as a result of their laminar flow and fast thermal response times. Mechanically, this occurs because the catalyst temperature – which typically lines the lower three walls of the microchannels and the microreactor itself – can be controlled within greater precision than in conventional reactors, as almost all of the heat loss of the microsystem occurs through its thin top walls. Varying the thickness and thermal conductivity of this wall, dissipation of the heat of reaction can be effectively controlled. In practice, this significantly dampens the overshoot and decay of temperature in feedback control loops, allowing the use of more extreme reaction conditions (Ehrfeld 2000).

- Costs of Scale-Up and Application: In microsystems, the connection of multiple well-stirred microreactors (functionally a set of CSTRs) in parallel – known as

"numbering up" – is essential to the design of μTAS. Despite the advantages of such systems, they exhibit diminishing economies of scale, as the microfabrication and precision engineering of microreactors in parallel costs more than the production of an equally productive conventional reactor typically. However, these diminishing economies of scale are compensated by any of the aforementioned benefits of using microreactors, such as using continuous flow rather than batch reactors, higher selectivity and conversion, less required catalyst, or improved heat and mass transfer properties (Ehrfeld 2000).

- Safety of Microsystems: Several safety-oriented advantages of microreactors have already been mentioned, such as the ability to operate under highly exothermic conditions or within explosive limits. By virtue of the multichannel and serial organization of microsystems, sensors can be placed to immediately detect the failure of individual microreactors. Microreactors, which release potentially dangerous chemicals at significantly lower levels than conventional reactors due to the difference in size, could be efficiently isolated and replaced without disrupting the entire microsystem. Furthermore, point-of-use microreactor fabrication is much more feasible, i.e. microsystems are far easier to create on-site as opposed to being shipped from other locations, which limits the need to transport and store reactive or hazardous chemicals (Ehrfeld 2000).

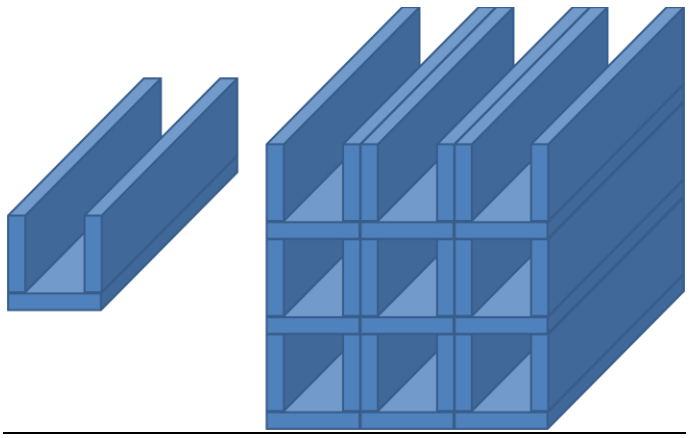

Figure 1: Through the connection of microchannels in ordered arrays and catalyst application onto their surfaces, microreactors are formed. The process of "numbering up" creates stacks of microchannels that are connected in series (not shown) to form μTAS, making favorable heat & mass transfer properties essential for the reactor material.

- Mixing: In liquid microreactors, mixing occurs primarily through diffusion as a result of their small scale and the properties of a laminar flow passing through them. As a result, there is more opportunity for phase transfer and separation.

The diffusion length must however retain its small size. This is typically done by running multiple microchannels of fluid next to one another, separated into several rows along a line parallel to their interfacial mixing zone. Upon combination, the diffusion length will be reduced in inverse proportion to the number of streams combined this way, rapidly mixing the streams prior to reaction (Jensen 2001).

- Concerns of Kinetic Properties and Production: Given that the microreactors themselves are produced on the micro rather than the nano scale, the general kinetic relationships governing reaction networks remain unaffected. Despite this, slight to moderate levels of noise may be present in concentration levels, reflecting the discrete nature of the chemical reactions in the system and justifying the use of kinetic Monte Carlo (KMC) methods in modeling feedback control. Resulting from the highly efficient mass transfer and absence of major flow irregularities in microsystems, the measurement of the kinetic properties of a microreactor is more accurate than that of a conventional one (Jensen 2001).

1.3 A Selection of Applications of μTAS *and Microreactors*

Currently, microreactors are applied to a wide range of disciplines in industry and academia; these applications range from high throughput screening and combinatorial chemistry in pharmaceuticals to the fabrication of Micro-electromechanical systems (MEMS) in electrical engineering. Within the domain of chemical engineering, there are more applications of microreactors in analysis and reaction systems than can be suitably explained here. Listed below are several specific chemical engineering applications of microreactors that have already been put into practice or are particularly promising:

- The partial oxidation of an isooctane liquid hydrocarbon feed in a fixed-bed microreactor, with the intent of producing hydrogen gas via other fuel reformation reactions, using one of several noble-metal based catalysts (e.g.: Pt-CeO_2). A kinetic model has been established using a Langmuir-Hinschelwood-Hougen-Watson (LHHW) formulation and the water-gas shift (WGS) reaction that

converts carbon monoxide and water into carbon dioxide and hydrogen gas has been taken into account (Pacheco 2003).

- A pulse microreactor-chromatograph is used in an analysis system to study the diffusion, adsorption, and reaction kinetics of the isomerization of xylene into its ortho, meta, and para-substituted forms, in addition to conversion into toluene. The dynamic analysis used to account for all of these processes occurs over a HZSM-5 zeolite catalyst, and the rate constants and activation energies of the Arrhenius form reaction rate expressions are determined with it (Li 1992).

- The production of dilute hydrogen peroxide (H_2O_2) through direct combination of H_2 and O_2 in a gaseous microreactor at typically flammable H_2 concentrations. The conventional anthraquinone autoxidation (AO) method used to produce H_2O_2 is not typically cost effective unless higher concentrations of H_2O_2 are produced due to transportation expenses, which are reduced via point-of-use synthesis of μTAS (Voloshin 2007). In similar studies conducted within the explosive regime, Pt and Al_2O_3 were tested for suitability as catalysts for this reaction (Hessel 2005).

- In another study, the HZSM-5 zeolite catalyst is used in a purely reaction kinetic study of methanol conversion to light olefins in a membrane microreactor using the SAPO-34 molecular sieve. This reaction network, ultimately useful for modeling the catalytic formation of paraffins, considers the deactivating effects of carbon coke formation, the effects of methanol partial pressure, and other factors typically absent from pure Arrhenius expressions of rate equations (Chen 1999).

- A comprehensive summary of many kinetic models and reaction networks planned for synthesis in microreactors is performed in a review conducted by Watts and Wiles. Among liquid phase pressure-driven microreactors, diazonium salt synthesis, esterification of boc-glycine, Swern oxidations, are several of the many reactions referred to and reviewed. Electrochemical synthetic and gas-liquid phase reactions are also considered in this review (Watts 2006).

1.4.1 Overview of Production Techniques – Structuring

In the mass production of μTAS and microreactors, the most pressing issue of technical feasibility is microfabrication cost, stemming from the specialized methods and amount of material required to produce them. For mid to large-scale microreactors – the microchannel hydraulic diameters of which range from 100-500 μm – metals are the most common manufacturing material. Typically, these metals are stainless steel alloys, with compositions dictated by the operating temperature and other conditions of their contained reactions. High temperature applications, such as hydrocarbon reforming with the WGS reaction and partial oxidation, frequently use Ni or FeCrAl alloys, the latter of which is desirable also for the unique method by which catalyst coatings are applied to its inner surface. For lower temperature applications that require isothermal operating conditions, such as alcohol reformation and gas purification, Cu and Al are more suitable, with thermal conductivities (k) of 401 and 236 W/m×K, respectively. For reference, stainless steel has a k of approximately 15 W/m×K (Hessel 2005).

However, for smaller devices on the order of microelectromechanical machines (MEMS), or with microchannel D_h of less than 100 μm, quartz, polymers, ceramics, and glass can be used in high temperature applications (Watts 2006). The most common material for the uppermost layer of microreactors and microchannels surfaces is Si_3N_4 due to its temperature insulation effects, while the remaining parts of both are made from Si for its high heat conductivity (Hessel 2005). Though the insulation provided by Si_3N_4 is typically favorable, as the catalyst become thermally isolated and power no longer needs to be supplied to it following reactor ignition, microreactor operation in this autothermal mode is impractical in applications involving temperature control. For reactions that reach steady state at intermediate temperatures, such as the hydrogenation and dehydrogenation of cyclohexene, their selectivities cannot be maximized when conditions such as flow rate and the surrounding temperature are varied (Jensen 2001). Even without this insulation wall, temperature control remains problematic due to the extremely high h values of the pure Si channels (~41,000 W/m^2×K), leading to excessive heat dissipation. In order to minimize energy losses resulting from this, microreactors and microchannels are typically manufactured from Si-rich materials with less insulation, such as borosilicate glass, soda-lime-silica glass, PDMS, and PMMA (Watts 2006).

Aware of the materials from which MEMS-scale microreactors can be fabricated, a number of mass manufacturing methods can be considered for. Several fabrication methods, although effective in laboratory settings or on conventional reactors, are not suitable for the mass manufacture of microreactors with D_h below 100 μm, including:

- Micro electric discharge machining (μ-EDM): Also known as spark machining or spark erosion, μ-EDM is a microfabrication process by which metals (conductive materials) or ceramics of sufficient potential difference can be shaped or patterned by current-induced erosion of their surfaces. The two primary methods used to accomplish this – wire-cutting and die-sinking – both implement a 'tool' electrode to carry current (via electric breakdown) to a 'workpiece' electrode, the latter of which is to be refined, patterned, and shaped for application.
    - In the die-sinking method, the two electrodes are first submerged in an insulating or dielectric liquid, then the distance between them is varied, initiating electric breakdown in the form of sparks on the workpiece.
    - In the wire-cutting method, the two electrodes are connected by a thin, single wire (typically a brass wire of 20 μm) and are submerged in a dielectric fluid. Current is induced through the wire, which moves in order to etch patterns on the surface or interior of the workpiece.

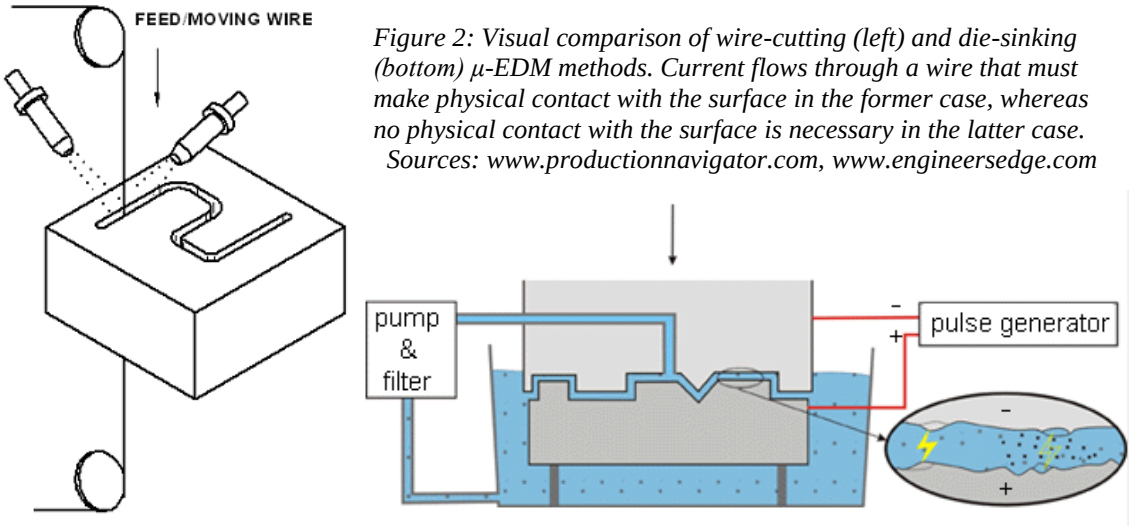

Figure 2: Visual comparison of wire-cutting (left) and die-sinking (bottom) μ-EDM methods. Current flows through a wire that must make physical contact with the surface in the former case, whereas no physical contact with the surface is necessary in the latter case. Sources: www.productionnavigator.com, www.engineersedge.com

- The geometries generated on the workpiece can be highly complex regardless of the workpiece's mechanical or material properties, rendering μ-EDM suitable for

microreactor materials that are chemically resistive, hard, or have larger grain sizes. In addition, the lack of material contact significantly reduces the cost of cleaning eroded edges of burr, and patterns can be etched into surfaces of high aspect ratio. Despite these benefits, however, they are not cost effective in mass microfabrication and are limited in their precision by the diameter of the wire or the nature of the fluid in which they are submerged (Hessel 2005).

- Micro-milling: Similar to its conventional counterpart, micro-milling involves the physical pulverization of materials that have already been crushed into more refined shapes via physical impact. Proven effective in generating architectures of or below 100 μm, micro milled structures often need further drilling, turning, and sawing to become useful for application. Primarily, micro-milling is effective in producing parallel microchannels from iron or aluminum, which require ceramic or monocrystalline diamond beaters to structure them, respectively. Due to the equipment needed and difficulties in accurately replicating microchannels, micro-milling is typically not considered in industrial applications (Hessel 2005).

- Micro-punching: A technique typically used in metalworking, micro-punching can be described as the use of a pressurized drill to create holes and indentations in a substrate, typically made of metal. Despite its reliability, reproducibility, and low cost in mass production, most industrial drill bits are limited in creating channels several hundred micrometers wide, and are accurate to within 50 μm. In addition, punching techniques are generally only capable of producing straight channel systems, which is a limiting factor when considering integration into μTAS that implement non-cross flow heat exchangers. Thus, micro-punching is too limiting for systems that would require KMC control (Hessel 2005).

Beyond technologies that are impractical for mass microfabrication below 100 μm, there exists several etching techniques applicable to microreactor manufacturing that resemble those used in Si wafer photolithography. These include wet (chemical) and dry (plasma) etching processes, both of which involve subjecting a material surface to UV radiation after applying a resistive mask over it, the mask itself being patterned to

generate the contour of the microchannel. In the former case, the exposed surface is eroded by a chemical solution such as $FeCl_3$ or HF, whereas a low pressure plasma or ion beam is implemented in the latter (Hessel 2005). Specifically, these microfabrication techniques are applicable to μTAS and microreactors as follows:

- Isotropic wet chemical etching: typically used to pattern metal foils, isotropic etching erodes the silicon surface uniformly in every direction. As a result, it eliminates surface material underneath the restrictive mask and produces a nearly cylindrical channel. This contouring, which cannot be controlled, is subject to severe limitations, such as its imprecision at length scales less than 300 μm. More importantly, only smaller aspect ratios can be etched isotropically; channels with significantly greater depth than length will be structurally unstable (the side walls will be eroded entirely), while those with much larger widths will waste material. As a result, isotropic wet etching is inadequate for MEMS-scale microreactor fabrication (Ehrfeld 2000).

- Anisotropic wet chemical etching: Originally developed from the micromachining of both bulk and surface single-crystalline silicon, anisotropic etching features chemicals (KOH, SbF_6, HF, etc.) that erode at different velocities with respect to crystalline direction. Etching velocity, now a function of radial direction, can be controlled such that Si underneath the UV mask remains unaffected and different channel geometries can be created. Even though it is significantly more costly than isotropic etching and requires a clean room, automation is cost-effective for small-series production. With the newfound precision control offered by anisotropic etching, batch processing can create several different structures on a single wafer in parallel, such as grooves, channels, cantilevers, pumps, valves, and static mixers. The construction of several of these analytical components on a single wafer can significantly reduce manufacturing costs, as will be shown later (Ehrfeld 2000). Thus, anisotropic wet chemical etching is the first viable microfabrication option introduced here, offering advantages such as:
    - Easy combination with thin films, sensors, heaters, and catalysts

- Makes irreversible microstructured Si-rich layers that simplify process control of catalytic reactions by mostly removing material limitations such as corrosion and leakage
- Benefits from thermal and anodic bonding processes (Ehrfeld 2000)

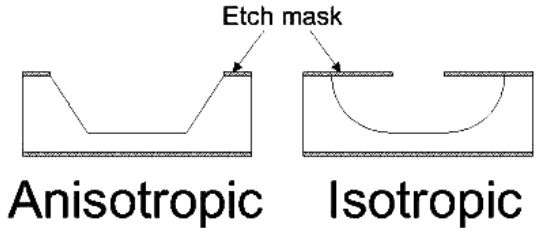

Figure 3: The difference between isotropic and anisotropic etchants visualized. Note that the walls generated by anisotropic wet etching cannot be entirely perpendicular to the substrate, as the etchant would have no horizontal velocity component.

Source: https://www.memsnet.org/

- Dry chemical etching: Instead of applying an aqueous chemical solution to etch the surface, dry chemical etching implements either low pressure plasma or reactive ion beams under ultra-high vacuum (UHV) conditions. This highly anisotropic removal of material has several advantages over wet etching, such as fewer geometrical restrictions, better resolution, and a wider choice of usable materials. These advantages are even more pronounced when a subset of dry etching, or Deep Reactive Ion Etching (DRIE), is used, which renders structures with even higher aspect ratios at low temperatures (Ehrfeld 2000). However, these processes are not conducive to cost-effective serial production, and thus are not useable for microreactor fabrication. Nevertheless, DRIE remains an effective, precise method for producing the patterned UV masks used as a template for microchannel patterning (Watts 2006).

Several other cost effective and technologically viable methods exist for the mass production of microchannels with D_h lower than 100 μm, including:

- Soft Lithography: Though referring to an assortment of techniques, soft lithography frequently integrates the processes of microinjection molding and hot embossing to generate microstructures. The process of hot embossing first heats an elastomer (elastic polymer) such as PDMS or poly(dimethylsiloxane) above its glass transition temperature (T_g), then presses a template of a microchannel (generated by DRIE or a similar process) into the elastomer. After cooling both

down, the elastomer becomes a mold of the template ready for on-site self-replication via microinjection molding or a related process. Microinjection molding then inserts a heated liquid mass of the desired microreactor material into the mold, which will solidify to form the reactors themselves. Several advantages exist in using soft lithography technology, including (Ehrfeld 2000):

  - Rapid replication through a template is one of the least expensive, viable options available for making microchannels with D_h less than 100 μm
  - Can be used for the fabrication of mixed ceramic, polymeric, and metallic-based μTAS (Watts 2006)
  - Mass produces high-quality features reliably (Hessel 2005)

- However, several limitations also exist in the use of soft lithography technology, none of which are insurmountable, rendering soft lithography a viable solution for MEMS-scale microchannel synthesis. These include:
  - The mold (typically PDMS) must have higher glass transition and melting temperatures than that of the channel material
  - In microinjection molding, the required size of the needle used to insert the replicated channel limits the fabrication of sub-micrometer features
  - Common, inexpensive mold materials such as PDMS usually swell in the presence of organic solvents and have limited temperature stability
    - Therefore, the microchannels will possess the same temperature limitations as the mold material (Ehrfeld 2000)
  - The integration of similarly scaled heat exchanges and controllers becomes challenging, even in laboratory settings (Hessel 2005)

- Laser ablation: In the context of micromachining, laser ablation implements a pulse laser to heat undesired sections of a solid material, which absorb the energy and sublime. Though generally considered infeasible due to cost, laser ablation has become economically viable for small-scale mass production of features below 100 μm. For microchannel applications that would require KMC control of reaction kinetics, this is a viable solution, though it is typically more cost effective when integrated with other production methods such as LIGA (Hessel 2005).

- Deep lithography + electroforming and molding (LIGA process): One of the most advanced microfabrication technologies, LIGA (Lithographie, Galvanoformung, Abformtechnik) is a refined combination of several of the methods presented previously. Initially, microchannels are formed by photolithography, and are subjected to an energy source determined by a trade-off between production cost and resolution of featuers. In order of increasing resolution and cost, typical energy sources include standard UV radiation, X-ray radiation, high-energy electron or ion beams, and lasers. After the photoresisting mask is removed, the Si-rich contoured substrate is used to generate a metal template via electroforming, or the deposition of Ni, Cu, or Au into the eroded contours of the substrate via an electrolytic reaction between the metal (cathode) and an ionized etchant solution (anode). Lastly, the mold created in this fashion is subjected to microinjection molding or a related process to mass manufacture microchannels. Within the domain of D_h below 100 μm, UV or X-ray radiation would be suitable, and subject to the following advantages and limitations (Ehrfeld 2000):
- Advantages:
    - Aspect ratios on the order of 100:1 with high qualitative surface quality, structural details on the μm scale can be replicated over centimeters
    - Micropumps and control devices have already been integrated into LIGA, accompanied with ceramic binders
    - Channel walls can be made more closely perpendicular (~89.95°) to their substrate (more rectangular) than can be realized in wet etching methods
    - Materials such as metals, metallic alloys, ceramics, and polymers can be used, though non-metals have limitations in mass production
    - The temperature tolerance of the mold, which is now composed of metal, does not limit that of the MEMS-scale devices (Ehrfeld 2000)
- Limitations:
    - Polymer-binded ceramics are limited by sintering and warpage in quality
    - Surface roughness cannot be controlled on the micrometer scale
    - Difficulties associated with plating into non-metal molds:

- Voids, indicated by hydrogen bubble nucleation in etchant solution
- Chemical incompatibility between the Si-rich substrate and the electroplated metal is common
- Mechanical incompatibility between the metal plating and the substrate causes can cause loss of adhesion (Ehrfeld 2000)

1.4.2 Overview of Production Techniques – Bonding & Coating

Microreactors that require KMC control device implementation, namely those with reactor microchannels with hydraulic diameter of less than 100 μm, can only be manufactured in a cost effective fashion under specific conditions. Namely, the channels themselves must be manufactured from Si-rich materials – such as borosilicate glass, soda-lime-silica glass, PDMS, and PMMA – and can only be fabricated using soft lithography, anisotropic wet chemical etching, laser ablation, or the LIGA process. Reducing the selection of microfabrication method candidates to the former and latter as a result of microscopic resolution and implementation issues, the types of bonding techniques available for integration with μTAS systems are heavily limited. Typically, anodic bonding of borosilicate (Pyrex) glass covers is used for this purpose, but unless modified, this method is not cost effective for mass production (Hessel 2006).

In addition, gaskets are impractical due to the scale of the system, and all forms of welding (conventional, laser, electron beam, etc.) are cost ineffective as a result of the heat transfer and melting properties of the microchannel materials. Similar to non-precision welding methods, the low-cost methods of brazing and soldering are severely limited by the presence of heavy metal catalysts that are highly reactive at temperatures lower than the melting point of the microchannel material. Sintering, or the heating of powdered substrates at near-melting point temperatures to adhere them together, is also impractical due to the poor microscopic resolution generated by the technique. One of the few adequate techniques for this is diffusion bonding, in which a large contact pressure (on the order of several hundred bar) is applied to separate substrate materials at high temperature (50-80% of their melting point) and under UHV conditions (Hessel 2006). Through this technique, microchannels can be sealed irreversibly, but

interconnection of them must proceed through a special technique called microlamination (Ehrfeld 2006).

Similar to its macroscopic counterpart, microlamination interconnects several thin metal sheets (also known as shims or laminates) with thickness on the order of several hundred micrometers. These sheets, which can contain various microstructures such as heat exchangers, micropumps, and open channel systems, are usually fabricated through wet chemical etching and laser cutting rather than soft lithography (Ehrfeld 2006). There are few limitations on the types of materials that can be microlaminated, and the method has seen widespread use in fuel evaporation and reforming applications. Individual components of microreactors can be achieved by laminating pattered ceramic (Si) tapes, and three-dimensional architectures can be actualized through systemized stacking of multiple laminates. For these reasons, anisotropic wet chemical etching proves to be the most versatile of the industrial manufacturing methods presented thus far, considering such factors as cost, μTAS integration, and previous implementation (Jensen 2001).

Unlike microfabrication and bonding methods, which are highly limited by cost efficiency, feature resolution, and other factors, the coating of microchannels with catalytically active material can be pursued successfully through multiple methods for MEMS-scale devices. The coating process, which effectively creates microreactors from catalyst covered microchannels (Jensen 2001), is a more cost effective alternative to fabricating microchannels purely from the catalyst itself. In addition, it is required in industrial applications, as processes such as sputtering and chemical vapor deposition (CVD) do not generate enough surface area upon which catalysts can be deposited to achieve sufficient reactor productivity (Hessel 2006). Currently, three methods of coating are most widely seen in industrial applications (Ouyang 2003):

- Sol-gel Coating: The use of a sol-gel – a chemical solution formed into a gel by being subjected to several forms of hydrolysis and polycondensation – is convenient for coating microreactors by virtue of its low viscosity. As a result, low viscosity gels of titania (TiO_2), silica (SiO_2), and alumina (Al_2O_3) can be formed and simply pumped through the microchannels to coat them. Extensive research has been performed in optimizing this coating process for application in

industry, and has determined that the adhesion of the coat to the microchannel is greatly enhanced by the prior addition of a thin alumina layer. Cost minimization in this fashion, however, causes phase transition from alumina to corundum and sintering at high temperatures (~800 °C). As a result, the use of this highly cost effective method encourages the use of heavy, more expensive metal catalysts such as Pt and Pd; a common combination of coating layer and catalyst that can be applied to μTAS involving KMC controllers is Pt/Al_2O_3 (Hessel 2006).

- Anodic Oxidation: Through the use of an electrolytic cell – similar to that seen in μ-EDM – an amorphous hydrated alumina can be deposited onto a "workpiece" anode containing a microchannel array from an aluminum-based cathode. This arrangement, producing an array of hexagonal cells that contain a pore at their center, creates highly uniform coating layers with highly ordered pores. However, the exact oxidation method used in laboratories is cost ineffective for industry applications, and is modified appropriately. Specifically, the modifications entail the use of the aluminum alloy $AlMg_3$ on the cathode, the connection of the two electrodes with thin aluminum wires, and the impregnation of the catalyst carriers with Pt. With this reduction in process design cost, anodic oxidation is rendered an adequate method for the industrial coating of microreactors (Hessel 2006).

- Electrophoretic Deposition: Encompassing a larger range of coating techniques that coat microstructures with catalyst powders in industry, this process deposits particles suspended in a liquid colloid via induction from an electrical field. Similar to anodic oxidation, particles deposited onto the "workpiece" electrode and portions of the microchannels themselves must contain an inherent charge, a surmountable challenge in the case of Si-rich MEMS-scale devices. Most experimental work attempting to achieve this has involved the deposition of alumina and Pd layers. In the event that this requirement can be overcome, electrophoretic deposition has several advantages, such as high coating speed, high purity, and facile control of coating layer thickness (Hessel 2006).

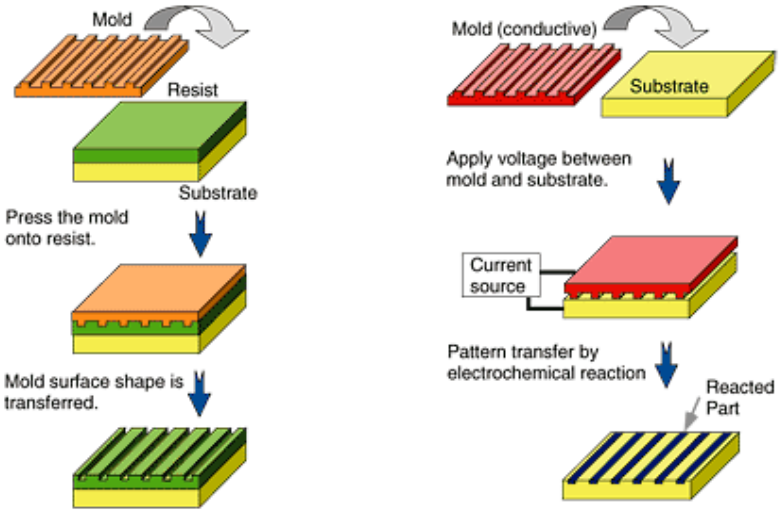

Figure 4: Implementation of soft lithography (left) hot embossing method and anodic oxidation (right) to pattern a substrate. The substrate masked with a photoresist is molded by physical means before photolithography and wet chemical etching are used to refine its features and remove the resist. Physical contact between the mold and the substrate is not necessary for anodic oxidation, as is seen here.

Source: www.ntt-review.jp

1.4.3: Overview of Production Techniques – Micropumps

Upon integration into μTAS that would require KMC controllers, accurate pumping mechanisms are required to provide information to the control software. Though many mechanisms exist that can accomplish this, they are typically classified as either mechanical or non-mechanical, the latter group containing the important subset of electrokinetic flow. Mechanical micropumps, which are generally powered by the movement of a membrane, deliver any type of fluid or gas in discrete units, usually leading to the disadvantage of pulsed rather than continuous flow. This can create non-uniform flow, leaking between the pump and the device, and higher dead volume, problems which are challenging to overcome. Non-mechanical pumps, on the other hand, have almost the exact opposite benefits and limitations. Based on the direct transfer of energy, they are continuous and employ capillary or evaporative forces that heavily reduce leaking, and involve no moving mechanical parts subject to breakdown. On the other hand, pump performance is almost entirely dictated by the nature of the fluid. Thus, non-mechanical micropumps are almost universally preferred, given that the feed stream has favorable properties such as low viscosity and density. Inasmuch as KMC control of the feed flow is concerned, electrokinetic field induced flow – which acts as both a valve and a pump – allows for control of both the direction and the magnitude of fluid flow, an advantageous feature that reduces leaks and thus process design costs (Watts 2006).

1.5 Project Charter

Project Charter Name	Model-Based Control with Stochastic Simulators: Building Process Design and Control Software for Catalytically Enhanced Microsystems
Project Champions	Dr. Talid R. Sinno
Project Leader(s)	Matthew T. Curnan, Arjun Gopalratnam, Charlie G. Slominski, Eric Wang
Specific Goals	Design a case study demonstrating the maximization of desired product yields and minimization of production costs in a setup comprised of multiple continuous, well-stirred microreactors regulated by a single multivariable model-based controller

Project Scope	In-scope:
	• Develop various general kMC models provided by SPPARKS, including:
	  o Basic A <–> B reaction model
	  o 2-D Ising Model, 3-D Potts Model (generalization of Ising)
	  o 2-D Particle Deposition Model (subset of Diffusion application)
	• Introduce the optimal temperature control problem to the general A <–> B reaction model, reproducing continuum results produced in MATLAB
	• Observe the effects of reducing feature length to promote stochasticity and discrete molecular reactions while varying process parameters
	• Design a model-based controller capable of reducing stochastic noise in concentration values for a constant set point temperature
	• Model the competing hydrogenation and dehydrogenation reactions of C_6H_{10} (cyclohexene) over a series of well-stirred microreactors, controlling the stochasticity of each CSTR such that they approach continuum PFR behavior
	Out-of-scope:
	• Quantitative analysis of the effects of introducing different microchannel components, surface catalysts, and geometries
	• Alternative surface reactions (adhesion, non-nearest member adsorption, etc.) that affect dehydrogenation and hydrogenation on the catalyzed surface
	• Design costs in μTAS microfabrication, excluding manufacture and control

Deliverables	• A computational framework consisting of the following parts:
	  o A multivariable feedback closed control loop governing temperature within the microreactor over time
	  o A stochastic model of the dehydrogenation / hydrogenation reaction kinetics within each microreactor provided via SPPARKS
	  o A PHP-generated script linking the aforementioned to form a system of CSTRs in series, functionally modeling a stochastic PFR
	  o A graphical user interface (GUI) for parameter modification

Time Line	• January 31st: Completed preliminary designs (observing relationships between process variables, become proficient in general models) • February 28th: Process synthesis (modeling the stochasticity provided by SPPARKS, the optimal temperature problem, and model-based control) • March 31st: Design work (implementing the specific case studies, such as hydrogenation / dehydrogenation of cyclohexene and PFR modeling) • April 9th / 16th: Rough Draft / Final Draft of Report Due • April 20th: Oral Presentation of Results

1.6 Innovation Map

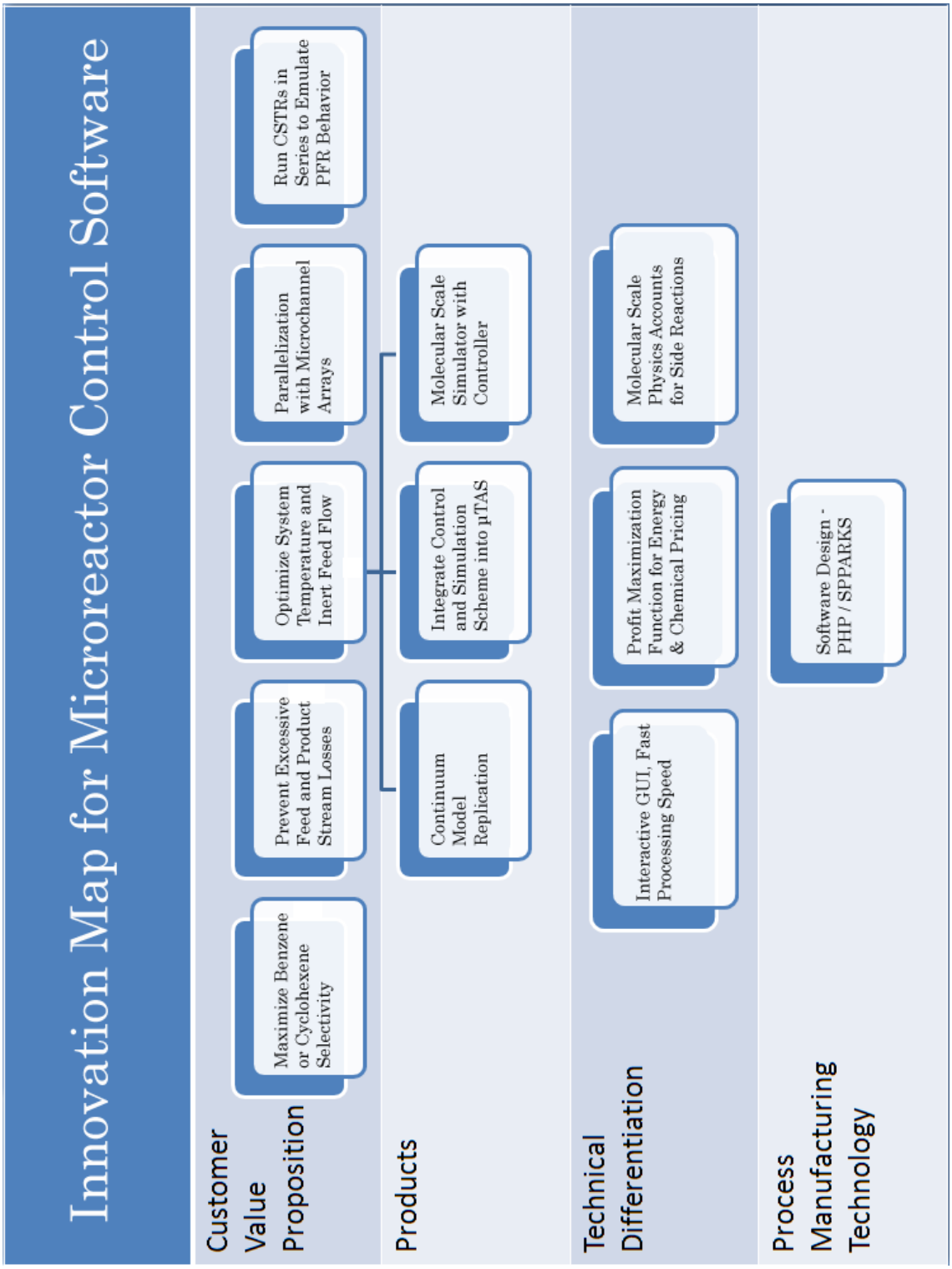

2 Method of Solution

2.1 Modeled Reactor Types

Microreactors are generally continuous-flow reactors, as opposed to batch reactors, since continuous-flow reactors achieve higher throughputs, convert material faster, transfer heat faster, can be better optimized, and do not need to be emptied and refilled. Continuous-flow reactors are either tubular or duct reactors, or continuous tank reactors. Tubular or duct reactors are the preferred microstructure since they require less total volume, are more spread out, are more easily stacked, are better controlled, and simultaneously transport material further than continuous tank reactors. A common microreactor structure is shown in Figure 5.

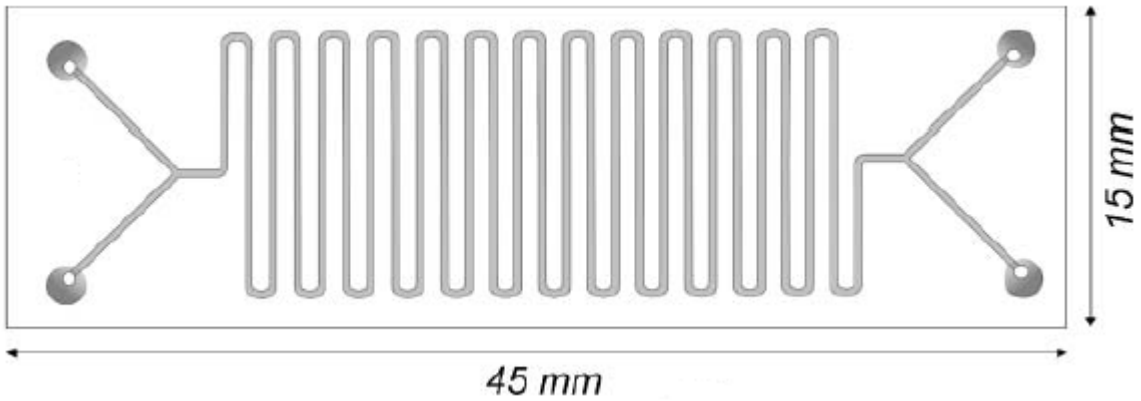

Figure 5 shows a common microreactor design (Znidarsic-Plazl 2007). Two reactants enter from different wells on the left, are mixed at the Y-shaped junction, then react along the length of the reactor. The product stream is divided into two and sent to different outlets.

While flow through microreactors can be simulated with computational fluid dynamics, such rigor is often unnecessary. In this study, a microreactor of fixed volume is modeled using a single continuous stirred-tank reactor (CSTR) or series of CSTRs, also referred to as the tanks-in-a-series model. A depiction of these two models is shown in Figure 6. The plug flow reactor model is achieved in the limit of an infinite number of tanks with infinitesimal volume. The serpentine structure and fast relative rate of diffusion at small length scales justifies the assumption of perfect mixing in these models.

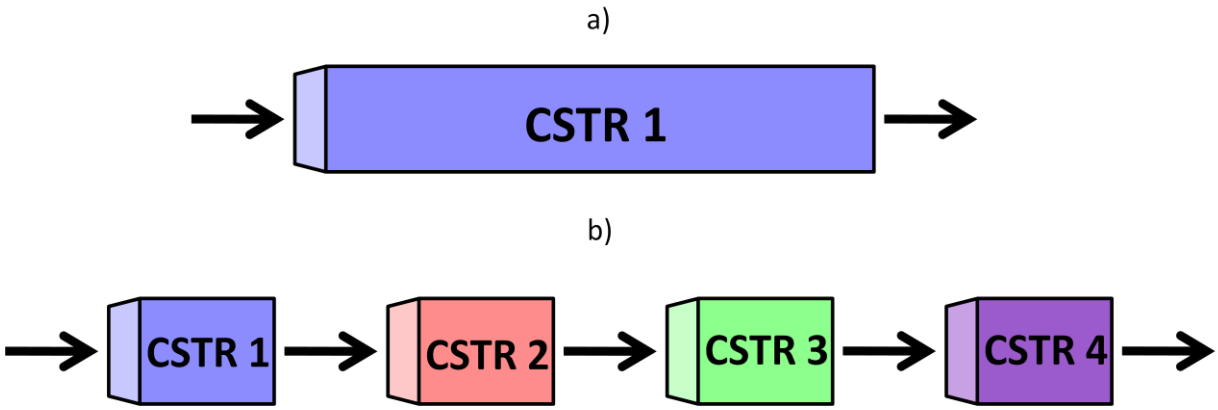

Figure 6a) shows a single CSTR model while Figure 6b shows the tanks-in-a-series model for four tanks. The total volume is the same in both models.

2.2 Stochastic Processes

A deterministic process is a process whose outcome is determined. The solutions of ordinary differential equations with initial conditions and partial differential equations with boundary values are examples of deterministic processes. On the contrary, stochastic processes are inherently random processes whose outcomes can differ each time the process is executed for a given set of parameters. While all real processes involve some degree of stochasticity, it can often be ignored when a large number of discrete elements are present. Any process involving a relatively small number of discrete elements where the occurrence of a single event is significant is stochastic. The stochastic process examined in this study is the kinetic behavior of a relatively small number of molecules. Other stochastic processes include the growth of a thin film in a surface deposition process, the risk of assets in a stock portfolio, the medical statistics of rare diseases, and roulette.

2.3 The Kinetic Monte Carlo Method

The Kinetic Monte Carlo (KMC) method is used to simulate models of stochastic processes (Gillespie 1992). Process parameters and initial conditions are specified at the beginning of the simulation. For the i^{th} time, the rate of each process, r_{ij}, corresponding to the event w_j, is computed. The total rate for the i^{th} time, R_i, is calculated by summing the individual rates:

$$R_i = \sum_{j=1}^{M} r_{ij}$$

where M is the number of processes. The probability that the ith process will occur is entered into a vector, P, where:

$$P_1 = 0$$

and

$$P_{j+1} = \frac{r_j}{R} + P_j$$

To determine which event happens over the current time step, a random number, $u_1 \in (0,1)$, is chosen using a random number generator. Then a binary search is performed on the vector P to find P_k such that $P_{k-1} < u_1 \leq P_k$. The event w_{k-1} corresponding to P_k is chosen to occur. A representation of this process is shown in Figure 7.

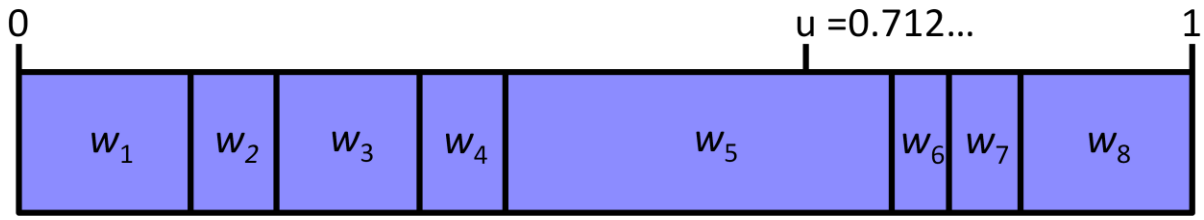

Figure 7 gives an example of how events are selected in a KMC simulation. For every time step, each event is assigned a probability equal to the ratio of its rate to the sum of the rates of all the events for that time step. Each event is given a range on the interval (0,1) corresponding to the probability it will be selected. Then a random number is selected on the interval (0,1). The event corresponding to the range in which the random number falls is chosen for that time step.

To determine how long of a time step to take, another random number, $u_2 \in (0,1)$, is chosen. It can be shown that the time step for a KMC simulation is (Gillespie 1992):

$$\Delta t = -\frac{\ln(u_2)}{R}$$

To better understand this time step, consider that the expected value of $-\ln(u_2)$ is 1. The system time is incremented by Δt following the selection of an event and its time:

$$t_{j+1} = t_j + \Delta t$$

It should be noted that the time step is chosen independently of which event is chosen. This algorithm is iterated until the system passes a fixed time or is determined to be at steady state.

2.4 SPPARKS

SPPARKS (Stochastic Parallel PARticle Kinetic Simulator) is a Monte Carlo code developed by Steve Plimpton, Aidan Thompson, and Alex Slepoy at Sandia National Laboratories. The code is written in C++ and can be run on a number of platforms on a single processor or in parallel on multiple processors and/or machines. SPPARKS is an open source code distributed under the terms of the GNU General Public License (GPL).

SPPARKS includes kinetic Monte Carlo (KMC), rejection kinetic Monte Carlo (rKMC), and Metropolis Monte Carlo (MMC) algorithms. An application, either packaged with SPPARKS or added by the user, defines events and their probabilities and, together with a solver or a sweeper, determines the evolution of the system. Instructions for setting up a simulation and select details are presented in Appendix A.

2.5 Description of the Numerical Method

A KMC simulation was set up in SPPARKS for each run. To achieve a CSTR model, an appropriate molecular flow rate was added and subtracted from the reactor after 0.2 seconds of each simulation elapsed, as shown in Figure 8. The inlet flow rate is specified in molecules/second, corresponding to a particular mass flow rate, $\dot{m}_{\text{in}}$. The outlet mass flow rate was set to be equal to the inlet mass flow rate:

$$\dot{m}_{\text{out}} = \dot{m}_{\text{in}}$$

Particles were removed in proportion to their mole fractions in the reactor as dictated by the ideal gas assumption. This led to negligible errors in the mass balance over time since the mass that needed to be removed from the reactor at each time step was not always possible given the mole fractions of the species in the reactor.

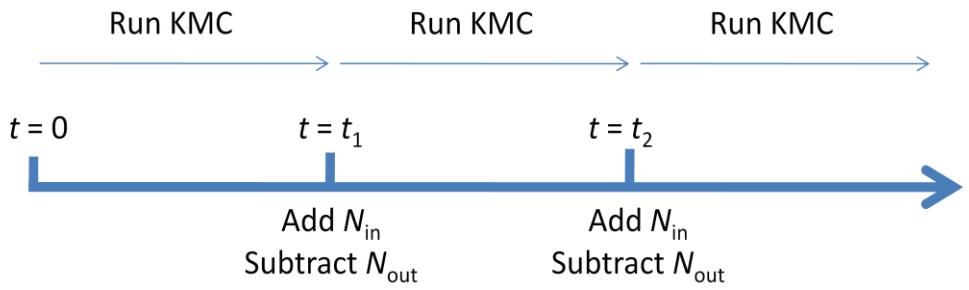

Figure 8 depicts the method used to add, remove, and react particles and to advance time.

2.6 Control Goals and Strategies

The control goals include maximizing and minimizing the outlet flow rates of the species involved in the reactions and their relative concentrations in the product stream. The goals were maximized by a model-predictive controller that was implemented at every time step. In the model predictive control strategy used in this report, two simulations were run at each time step. Initially, one simulation was run with a temperature 10 Kelvin higher than the base simulation and one was run with a temperature 10 Kelvin lower than the base simulation. The conditions of the simulation that better met the control goal were then implemented for the next time step of the base simulation. To increase the precision of the model predictive controller, the temperature change for the model predictive simulations was cut in half if the temperature returned to its value at the beginning of the previous time step. The temperature change was programmed to stay above 1 Kelvin and would reset to 10 Kelvin if the temperature changed monotonically. A schematic of the model predictive controller is shown in Figure 9.

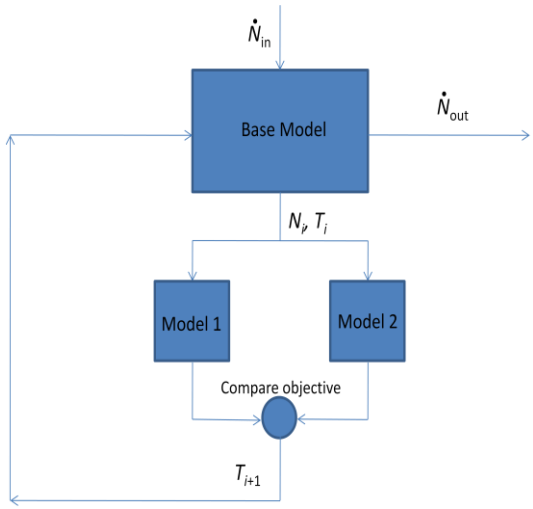

Figure 9 shows the model predictive control scheme implemented in this project. The current values of the base simulation are inputted into predictive models, which are run for a single time step. The temperature of the model which best meets the control objective is chosen for the next time step of the base model.

3 Control of Cyclohexene Hydrogenation and Dehydrogenation

3.1 Introduction to Catalyzed Hydrogenation and Dehydrogenation Reactions

The use of KMC model-based controllers in adequately scaled microreactors has been considered for several chemical reactions networks, one of which contains the competing hydrogenation and dehydrogenation reactions of cyclohexene (C_6H_{10}). In organic chemistry, a hydrogenation reaction can be defined as the addition of hydrogen (H_2) to an organic compound – such as a hydrocarbon – in order to saturate one of its double or triple bonds. Hydrogenation reactions typically occur on catalyst surfaces, thus *syn* or same-side addition of hydrogen atoms generally occurs across the unsaturated bond. Though mechanistically dissimilar to their complement, dehydrogenation reactions involve the removal of H_2 to unsaturate bonds and release hydrogen gas; in experimental work, the concentration of the released gas in a sealed chamber is frequently used to indicate rates of reaction and other kinetic information. The competing hydrogenation and dehydrogation reactions in this network are, respectively (Nassar 2006):

$$C_6H_{10} + H_2 \rightarrow C_6H_{12} \qquad (1; \text{represented by } k_1)$$

$$C_6H_{10} \rightarrow C_6H_6 + 2H_2\,(g) \qquad (2; \text{represented by } k_2)$$

Table 1: Rate constant and Energy of Activation Data for Cyclohexene Reaction Network

Reaction Type	k (L/min)	E_a (J/mol)
Hydrogenation (1)	218.	21,700
Dehydrogenation (2)	0.160	1920.

The rate equations governing these competing processes are generally Arrhenius in form; the hydrogenation reaction is second-order with respect to both cyclohexene and hydrogen, while the dehydrogenation reaction is first-order with respect to cyclohexene. They can be written as (Nasser 2006):

$$r_{\mathrm{d}} = \left(\frac{N_{\mathrm{C_6H_{10}}}}{VN_{avo}}\right) k_{\mathrm{d}} \exp\left(-\frac{E_{\mathrm{d}}}{\mathrm{R}T}\right)$$

$$r_{\mathrm{h}} = \left(\frac{N_{\mathrm{C_6H_{10}}}}{VN_{avo}}\right)\left(\frac{N_{\mathrm{H_2}}}{VN_{avo}}\right) k_{\mathrm{h}} \exp\left(-\frac{E_{\mathrm{h}}}{\mathrm{R}T}\right)$$

where r is the reaction rate in moles/liter-second, N_i is the number of molecules of type i, V is the volume in liters, N_{avo} is Avogadro's Number, $6.022*10^{23}$ molecules/mole, k_{d} is

the dehydrogenation reaction rate constant in 1/second, k_h is the hydrogenation reaction rate constant in liters/mole-second, *E* is the activation energy in joules, R is the gas constant, 8.314 joules/mole-Kelvin, and *T* is the temperature in Kelvin.

3.2 Description of Reaction Networks, Mechanisms, and Initial Catalysts

In addition to producing cyclohexane (C_6H_{12}) and benzene (C_6H_6), this network features several side reactions – such as the decomposition of benzene into graphitic or atomic carbon (Henn 1992) under extreme conditions (high temperature, pressure, etc.) and formation of 1,3 and 1,4-cyclohexadiene (Su 1999) – that can occur depending on catalyst, substrate, and pressure conditions. They are explicitly written, respectively, as:

$$C_6H_6 \rightarrow 6C_{(s)} + 3H_2(g) \quad (3)$$

$$C_6H_{10} \rightarrow C_6H_8 + H_2(g) \quad (4)$$

However, these reactions are not pursued in the KMC modeling of this network for several reasons. The formation of cyclohexadiene, which occurs only on some catalyst surfaces over limited temperature ranges, is a mechanistic intermediate in the catalytic surface chemistry of cyclohexene. Even though it affects the final concentration of benzene in the outlet stream of the microreactor mainly as a function of temperature, cyclohexadiene would either not be represented as a final product of the reaction network or only be present as a trace element due to the kinetic unfavorability of its desorption from the catalytic surface (Su 1999). Therefore, modeling this formation reaction would only be important on the scale of molecular deposition and not for general, equation-based reaction mechanisms. In the KMC control scheme implemented, noise in product concentration levels represents the discreteness of the process occurring in each microreactor that cannot be accounted for by continuum relationships. In attempting to control this noise in product concentration levels with temperature and inert gas flow rate, we are only concerned about factors that directly affect concentration control. Therefore, reactions such as the formation of cyclohexadiene, which only directly affect surface conditions such as roughness and film growth rate but not product selectivity or yields – are not included. The decomposition reaction of benzene, though not excluded from consideration, is avoided by keeping reactor temperature low (Xu 1994). In addition to

saving energy and thus reducing process design costs, the maintenance of a sufficiently low reactor temperature – specific to each catalyst surface – is maintained in all KMC simulations performed. However, none of these simulations account for the type of catalyst used because they do not account for surface conditions; therefore, the operating temperatures at which optimized reactions proceed in our simulations will either validate or invalidate the use of specific catalysts.

In industrial applications, hydrogenation and dehydrogenation reactions require control due to their exothermic nature and catalysts to increase their reactivity and yields. Though homogenous catalysts are implemented in laboratory settings due to their ease of use and simplicity, heterogeneous catalysts dominate industry due to their increased reliability, performance over time, and general prevention of undesired surface reactions. A critical first step to selecting a catalyst is to select an initial base (Ni, Cu, Co, etc.) or precious (Pt, Pd, Rh, etc.) homogenous metal to which solid state additives can be applied. In cases where temperature and pressure produce no physical or chemical disadvantages, Ni is generally the selected hydrogenating catalyst due to its proven reliability and cost efficiency relative to almost all other catalysts. However, for reactions occurring on a smaller scale that are sensitive to temperature – such as the hydrogenation of cyclohexene in a microreactor – more precious metals such as Pt are preferred for their greater selectivity at smaller loadings (0.5-1.0%) and less extreme required operating conditions (Rase 2000). To solidify this assumption, Rase recommends the precious metals Pd and Pt, along with the base metal Ni, as initial catalysts in olefin to alkane reactions or vice versa (Rase 2000). The particular selection of catalyst, in addition to specific questions regarding reaction mechanisms and kinetics, will be expounded upon later.

Regardless of the catalyst and surface conditions, this reaction network is heavily dependent on ambient temperature and pressure conditions. In an experimental study, the hydrogenation and dehydrogenation of cyclohexene was conducted on a Pt(223) surface while maintaining a temperature range of 25-150 °C. At UHV conditions (~10^{-7} torr), benzene selectivity predominated, whereas conditions closer to STP (~10^{2} torr) promoted greater cyclohexene selectivity (Davis 1980). In related research using a Pt/SiO_2 substrate and vapor phase hydrogenation of cyclohexene, a similar mechanistic shift was observed in varying temperature between 273 and 313 K, the first case favoring high cyclohexene yields and the second demonstrating greater benzene selectivity (Segal 1978). This kinetic shift results from the substrate independent Horiuti-Polanyi mechanism, shown in Figure 10, that governs cyclohexane selectivity. In this mechanism, the initiation step occurs as hydrogen gas first breaks down into hydrogen radicals and olefins (e.g.: cyclohexene) break their double bonds to form stable diradical molecules adsorbed to the catalytic surface. Increasing temperature causes desorption to occur, catalyzing the propagation step in which radical hydrogen molecules attach to the former olefins, resulting in termination when all active sites are consumed and benzene desorbs from the catalyst surface. Adsorption of hydrogen, which is equilibrated at higher temperatures and lower pressures, becomes irreversible at lower temperatures and higher pressures.

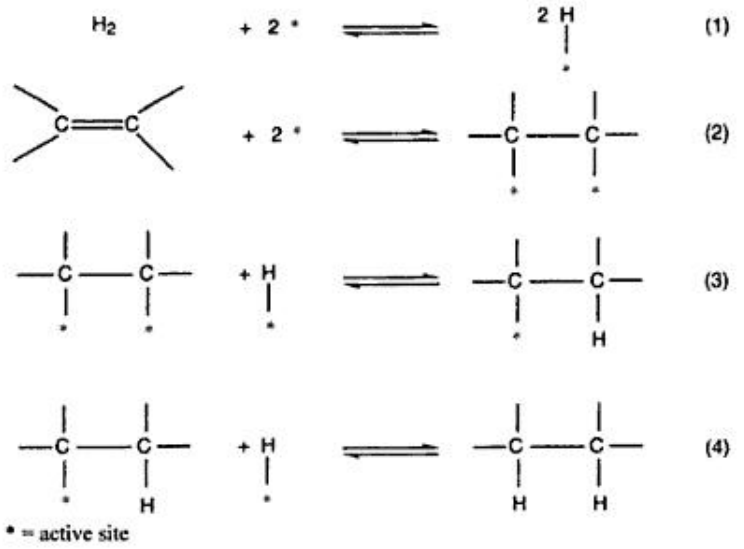

Figure 10: General, surface independent representation of the Horiuti-Polanyi mechanism. Source: Handbook of Commercial Catalysts: Heterogeneous Catalysts

Given this information and the mechanism below, the aforementioned kinetic shift results from the inability of radical hydrogen to reversibly bond with a cyclohexene intermediate formed on their mutually adsorbed surface, forcing it to desorb as cyclohexane at low temperatures or under insufficiently energetic conditions (Segal 1978).

For the lower temperature, higher pressure conditions that favor cyclohexene formation specified previously, structural insensitivity – or independence of surface chemistry on the concentrations of reaction – is found to be a very reasonable modeling assumption. On the other hand, structural sensitivity is noticeable under UHV conditions and at temperatures conducive to carbon coking (i.e.: graphitic atomic carbon formation) or optimal levels of benzene formation (Segal 1980), thus surface chemistry should be considered under these conditions. In order to understand the mechanism of cyclohexene hydrogenation in a surface specific fashion, a basic homogenous catalyst – Pt(111) – will be provided as an example due to its extensive use in hydrogenation reactions performed in laboratories and its role as a basis of comparison for other heterogenous catalysts. A prerequisite for cyclohexene conversion into another species in fluidic microchannels is adsorption onto their catalytic surface, which typically occurs at 95-100 K in the form of two singular σ-bonds between the now radical cyclohexene and the surface. When heated to 180-220 K, a C_6H_9 intermediate is formed on the surface, in which one radical bond of the aforementioned cyclohexene olefin intermediate bonds with a radical hydrogen atom while the other remains adsorbed to the surface. Currently, a "standing-up" conformation, as pictured in Figure 11, is hypothesized to accurately model the geometry of this intermediate on Pt(111), but more extensive research is being conducted on specific conformations of other financially viable homogenous and heterogeneous catalysts (Xu 1994).

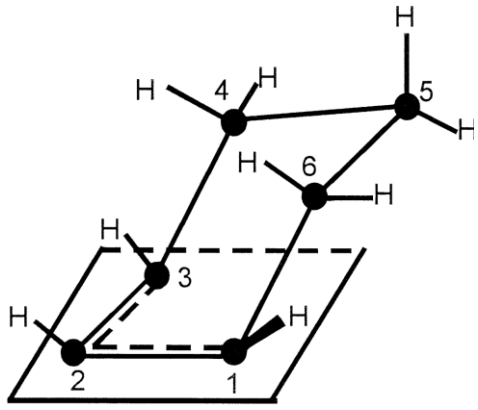

Figure 11: "Standing-up" conformation of the intermediate (multiple stable C_6H_9 resonance structures) that forms on Pt(111) surfaces, among other structures.
Source: (Su 1999)

At this point, cyclohexene develops several resonance structures, which occur in higher yields as temperature is increased beyond 220 K. These ultimately lead to the formation of benzene at approximately 300 K, though the specific reaction mechanism that enables this formation is still being studied (Xu 1994). Currently, it is hypothesized that the cyclohexene intermediate alternates between *cis* ("sitting-down") and *trans* ("standing-up") states on the surface of the catalyst, as shown in Figure 12. Intuitively, the *cis* conformation would be assumed more energetically favorable due to the lower steric interference caused by rendering an entire C_6H_9 complex parallel rather than perpendicular to the surface of the catalyst. Though this is true when the complex is being stabilized to the surface, the *trans* conformation becomes more stable when double bonds are being formed. This occurs because the hydrogen atoms, which would become radicalized once again upon desaturation of the complex, are close enough to the surface in the *trans* case to be readsorbed. The predominant resonance structures, which – at any given time – occur over the two unsaturated bonds closest to the surface, change as a double bond is added to the intermediate in its *trans* phase. The molecule, which rotated to change from *cis* to *trans* conformations in producing a single double bond, rotates once again in that same direction to produce a second *cis* state with resonance structures occurring over another two adjacent single bonds. This process, upon creating two more double bonds in an alternating pattern over four more single bonds, leads to desorption of the former intermediate (which is now the final product benzene) and reformation of the hydrogen radicals, which desorb from the surface as hydrogen gas. This entire process constitutes the dehydrogenation of cyclohexene on a catalyst surface (Henn 1992).

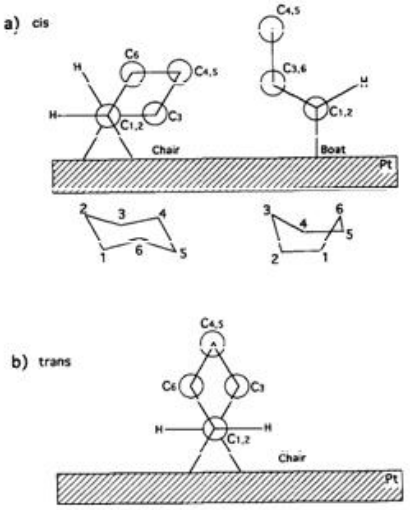

Figure 12: Visual Representation of the cis *and* trans *conformations of the C_6H_9 surface intermediate. Dehydrogenation is hypothesized to occur only in the* trans *case, while the intermediate adsorbs and stabilizes in the* cis *(i.e. syn addition) case to avoid steric interference. Source: (Xu 1994)*

The dehydrogenation process peaks at 350-400 K on Pt(111), at which the number of active sites on the catalyst is saturated at approximately 30% of its surface

area. Above 450-500 K, side reactions such as carbon coking induced by benzene decomposition have significant selectivity, rendering both main reaction rates lower and producing reaction conditions undesirable for industrial applications (Xu 1994). A summary of this primary reaction network, accounting for different cyclohexadiene forms of the surface intermediate (i.e.: double bonds located in different places on the cyclic complex) and favorable reaction conditions, is presented in Figure 13.

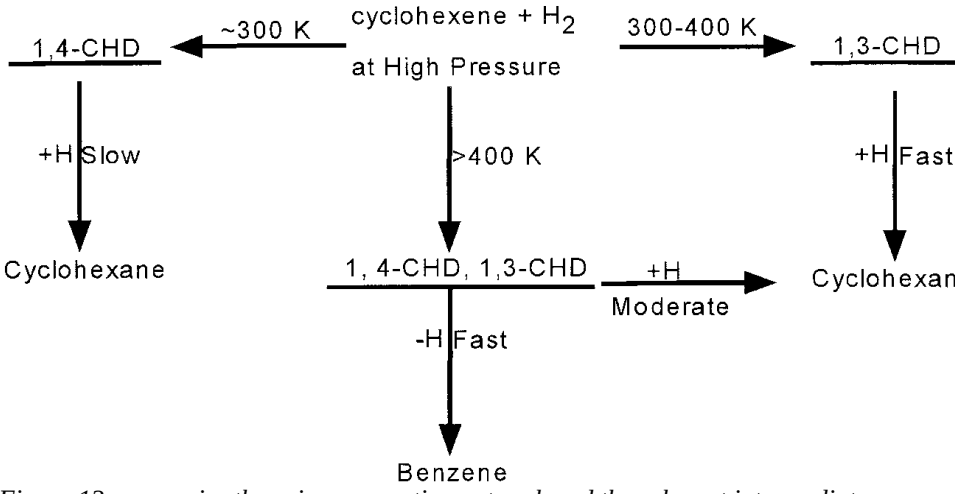

Figure 13 summaries the primary reaction network and the relevant intermediates.

3.3 Heterogenous Catalyst Analysis and Selection

As mentioned before, long-term exposure of a homogenous catalyst – such as Pt(111) – to adsorbed hydrocarbons eventually leads to the carbon coking on its surface, also known as carbon poisoning of its uppermost monolayer. To extend the lifetime of the catalytic metal and thus improve its application in industry, a second metal – such as Re, Ir, or Sn – or other additive is combined with it via a reformation reaction. The alloys formed in this fashion generally demonstrate greater aromatic selectivity, in addition to their primary purpose of avoided hydrocarbon side product formation. Prior to selecting candidates for heterogeneous catalysis in this reaction network, note that only alloys with Pt will be considered due to the inadequacy of the other initial catalysts – Pd and Ni – proposed by Rase (Rase 2000). The reaction mechanism for Pd(111) proceeds identically to that of Pt(111) up until 220 K, in which an intermediate is not appreciably formed on the catalyst surface and desorption of the hydrogenation product cyclohexane is almost

immediate at all temperatures below 400 K, after which decomposition of cyclohexene and cyclohexane induces carbon coking on the catalyst surface in significant quantities (Hunka 1999). Despite being used in ketone surface adsorption reactions, practical base metal catalysts such as Raney Nickel require higher operating temperatures and pressures than would be cost effective in the microchannels designed for μ-TAS control schemes (Chang 2000). Several heterogeneous Pt-alloyed catalysts have been considered and analyzed extensively in cyclohexene reaction networks, the additives of which typically change properties such as optimal dehydrogenation and hydrogenation temperatures and pressures by minimal amounts. They include:

- Sn / Pt(111) [Xu 1994]
- C / Mo(110) [Xu 1994]
- $x\mathrm{SiO_2} – (1 - x)\mathrm{Al_2O_3}$ / Pt(111) [Hassan 1995]

Of the three cases studied above, Sn / Pt(111) surface alloys have been studied the most extensively and have substantial benefits, such as not allowing the decomposition of benzene under UHV conditions. In addition, fewer layers of chemisorbed benzene on the alloy surface are needed to induce significant desorption rates from it, thereby improving the selectivity of benzene and reducing the time required to achieve high benzene yields. However, the optimal temperature for benzene selectivity under UHV conditions is increased to 400-450 K and decomposition occurs closer to 500 K, thus slight increases in process design costs result. Lastly, the presence of Sn in the catalyst has no effect on the adsorption kinetics of the reaction, implying that the kinetic models applied to the Pt(111) or surface insensitive reactions mentioned previously are still valid here (Xu 1994). Unlike the other two alloys or reformed metallic compounds, note that $x\mathrm{SiO_2} – (1 - x)\mathrm{Al_2O_3}$ / Pt(111) is in fact a carrier surface for Cobalt phthalocaynine (CoPc), which selectively enters silica pores on inclined edges and lies flat over alumina pores. This creates a variegated surface texture that hinders carbon coking differently depending on the concentrations of silica and alumina present on the surface (Hassan 1995).

4 Results of the Microreactor Simulations

4.1 Temperature Effects

The temperature was varied from 200 K to 600 K in steps of 100 K. In all simulations the microreactor was initially charged with argon and no argon was present in the inlet stream. Consequently, the concentration of argon in the reactor dropped to zero at steady state. Stochasticity was observed because a small number of particles (~1700) were present in the microreactor simulations. In the following figures, the dark blue, red, green, purple, and dashed light blue lines represent the number of molecules of cyclohexene, hydrogen, cyclohexane, benzene, and argon, respectively, while the orange line represents temperature. All simulations were performed with the initial conditions shown in Table 2. The maximum temperature was set to 600 K to avoid coking in the reactor and the minimum temperature was set to 200 K in order to achieve reasonably fast reaction rates.

Table 2 shows the initial conditions for the microreactor simulations.

Parameter	Value	Units
Initial Reactor contents	1000	Molecules of Argon
Flow rate	50	Molecules of Cyclohexene/second
Total Reactor Volume	10^{-20}	Liters

The simulation at 200 K is shown in Figure 14. A relatively large amount of cyclohexene accumulates in the reactor since the reaction rates are slow. Further, the largest concentration of hydrogen is seen because the hydrogenation reaction occurs relatively slowly at lower temperatures. Virtually no cyclohexane is present because it is produced in the hydrogenation reaction. Roughly twice as much hydrogen is observed as benzene. This indicates that the reaction is happening as expected because the stoichiometric ratio of hydrogen to benzene in the dehydrogenation reaction is two.

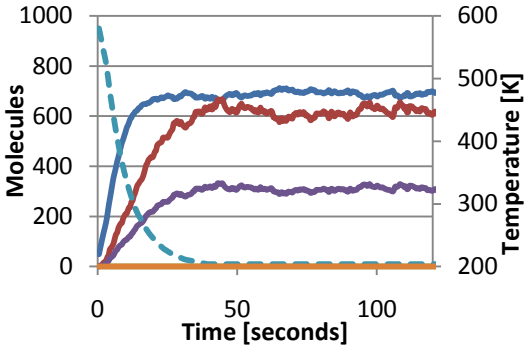

Figure 14 shows the contents of the CSTR when run at 200 K. The relative concentration of hydrogen was high when compared to other temperatures because the hydrogenation reaction occurs slowly at low temperatures.

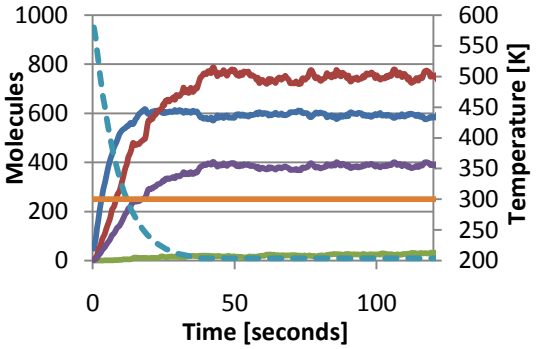

Figure 15 shows the contents of the CSTR when run at 300 K. The concentration of hydrogen decreased since the hydrogenation reaction occurred at an appreciable rate. The steady-state concentration of cyclohexene decreased from roughly 650 to 600 molecules because both rates of reaction increased.

Raising the temperature to 300 K did not significantly change the dynamics of the reactor, as shown in Figure 15. More cyclohexene was reacted since the increased temperature increased the contribution of the Arrhenius term to the rate equations. The ratio of hydrogen to benzene decreased from 2 to about 1.7 because more hydrogen was consumed in the hydrogenation reaction. The behavior of argon and the stochasticity were unaffected.

Raising the temperature to 600 K changed the dynamics of the reactor, as shown in Figure 16. The Arrhenius term for both reactions increased substantially so more cyclohexene was consumed. More cyclohexane was produced since more hydrogen was generated from the dehydrogenation reaction and the rate of the hydrogenation reaction increased. The behavior of Argon and the stochasticity of the simulation were unaffected. The outlet stream is equal parts cyclohexane, cyclohexene and benzene.

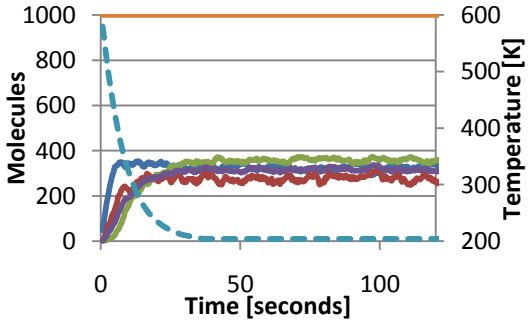

Figure 16 shows the contents of the CSTR at 600 K. The hydrogenation reaction proceeded much faster than at lower temperatures, decreasing the concentration of cyclohexane and hydrogen in the reactor while increasing that of benzene.

4.2 Tanks-in-a-series Approximation Results

The tanks-in-a-series approximation, as discussed in section 2.1, was tested. To maintain consistency between the simulations, the total volume of the microreactor system was kept constant while the number of CSTRs in series was increased. The volume of each CSTR was the total volume divided by the number of CSTRs in series. The simulation was designed such that the addition and removal of molecules from the CSTRs occurred in between periods of reaction.

The contents of the final reactor in each simulation are shown in Figure 17. Because the hydrogenation reaction requires hydrogen produced by the dehydrogenation reaction, the hydrogenation reaction occurs at a faster rate in the reactors that are further downstream. As a result, the concentration of cyclohexane in the final reactor increased with increasing CSTRs in series while the concentration of hydrogen decreased. The values in Figure 17 were multiplied by the number of CSTRs so that the contents of the final reactors were comparable between simulations despite their dissimilar volumes.

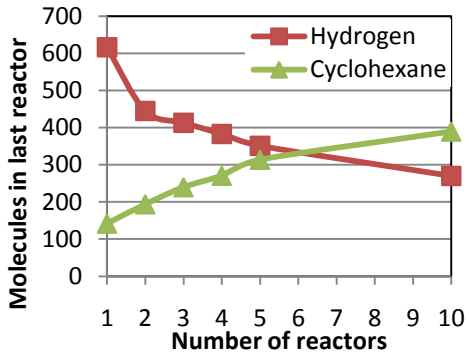

Figure 17 shows the contents of the microreactor system as the number of tanks in the tanks-in-a-series approximation is increased. The production of cyclohexane increases with the number of tanks.

4.3 Meeting Control Goals

The model predictive controller was applied to the reactor and a number of control objectives were specified. First, the ratio of benzene to cyclohexane was set to 1. Starting at an initial temperature of 400 K, the controller increased the temperature to 600K before settling around 560 K. The ratio of benzene to cyclohexane can be seen to be roughly 1 in Figure 18, as desired. The behavior of argon and the stochasticity of the simulation were unaffected. Running the simulation multiple times with different random number generator seeds lead to the same response, indicating that the model predictive controller was resistant to the stochasticity of the microreactor.

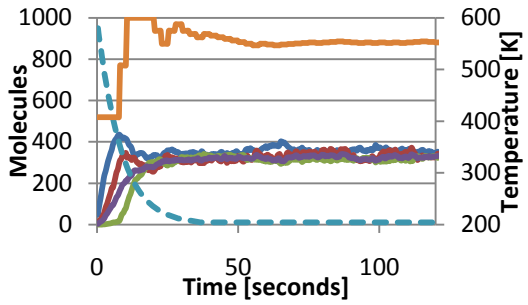

Figure 18 shows the controlled response of the CSTR when the ratio of benzene to cyclohexane in the effluent stream is set to 1.

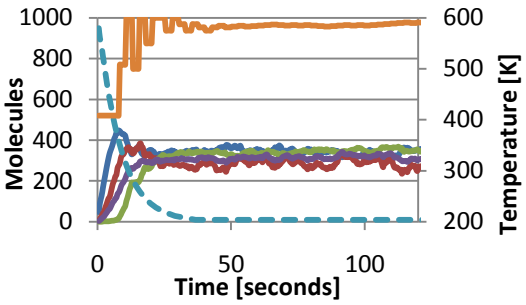

Figure 19 shows controlled response of the CSTR when the model predictive controller is set to maximize the effluent flow rate of benzene.

Next, the model predictive controller was set to maximize the amount of benzene in the effluent stream. The steady-state value for this control objective was found to be the maximum temperature of 600 K when starting from an initial temperature of 400 K. This is nearly the same temperature as that found for the previous control objective, indicating that the operating temperature where benzene is set to cyclohexane is also where the maximum flow rate of benzene is achieved. The transient and steady-state contents of the CSTR are shown in Figure 19. These results imply that separation of the products would be necessary if the production of benzene is maximized. Running the simulation multiple times with different random number seeds leads to the same response.

The model predictive controller was then set to maximize the amount of cyclohexane produced. The control behavior was nearly identical to that for the previous two control objectives. The results are shown in Figure 20. The model predictive controller was again found to be resistant to the stochasticity of the microreactor.

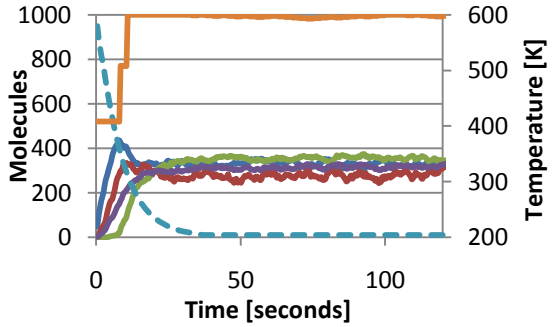

Figure 20 shows the contents of the CSTR when the concentration of cyclohexane is maximized. The temperature quickly rises to the maximum -- 600 K.

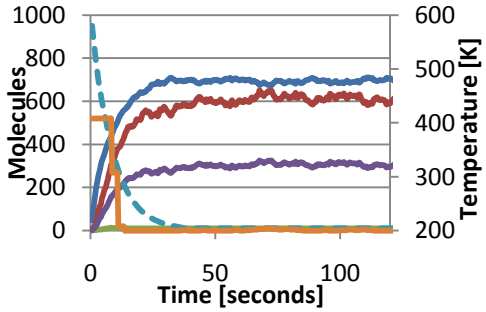

Figure 21 shows the behavior of the reactor when the outlet flow rate of cyclohexane is minimized. The temperature quickly drops off to the minimum temperature of 200 K.

Different behavior was observed when the flow rates of the two products were minimized. Figure 21 shows the behavior of the CSTR when the model predictive controller was set to minimize the flow rate of cyclohexane. The temperature quickly drops off to the minimum temperature allowed. At this temperature the Arrhenius term contributions to the reaction rates were small, causing less production of cyclohexane. The production of benzene was also minimized at 200 K.

The flow rate of hydrogen in the effluent stream was minimized at higher temperatures instead of lower temperatures. Figure 22 shows the behavior of the reactor when hydrogen is minimized. The temperature increases to 600 K from an initial temperature of 200 K. Hydrogen is minimized at higher temperatures because the hydrogenation reaction consumes more hydrogen than the dehydrogenation reaction produces as temperature is increased.

The temperature of the reactor once again dropped to 200 K when the ratio of benzene to cyclohexane was maximized. At this temperature the dehydrogenation proceeds slowly producing nearly no cyclohexane. This simulation's results are shown in Figure 23.

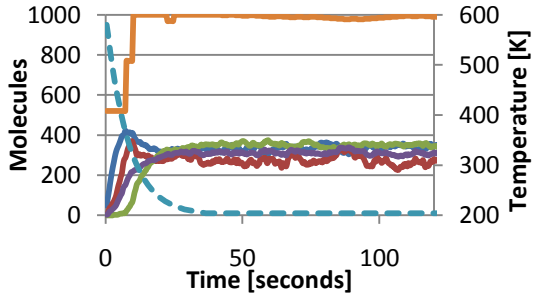

Figure 22 shows the behavior of the reactor when hydrogen is minimized. The steady-state temperature is 600 K.

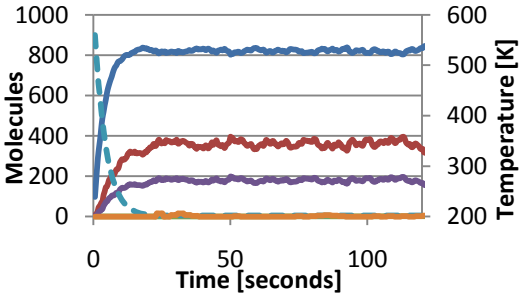

Figure 23 shows the behavior of the reactor when the ratio of benzene to cyclohexane is maximized. This occurs at 200 K when the dehydrogenation reaction proceeds slowly.

4.4 Conclusions of the Microreactor Simulations

The CSTR model incorporating a KMC batch reactor was able to carry out the simultaneous hydrogenation and dehydrogenation of cyclohexene accurately and with

reasonable stochasticity for the given reactor volumes. Future studies of the behavior of stochastic microreactors should look to use a similar model in their investigations.

The model predictive controller was able to meet its control objective while also being resistant to the inherent stochasticity of small scale microreactors. For this particular reaction network, the ratio of benzene to cyclohexane in the effluent approached unity and the production of cyclohexane and benzene were maximized at the maximum temperature of 600 K. Running the reactor above 600 K was undesirable because of the potential for clogging due to coking. At 200 K the hydrogenation proceeded extremely slowly producing very little benzene. Model predictive control incorporating additional manipulated variables, such as the flow rate of an inert species, could achieve greater specificity of the products and better control of the effluent stream.

5 Financial Analysis

5.1 Microreactor Market

Microreactors are not established units in industrial processes but have found some limited applications. For instance, China's Xi'an Huian Chemical is using microreactors to produce nitroglycerin at a rate of about 10 kilograms per hour, or about 97 short tons annually. Chemical companies Clariant, SAFC, BASF, Evonik Industries, DSM, and DuPont, pharmaceutical companies Schering-Plough, Sanofi Aventis, Roche, GlaxoSmithKline, Novartis, and Astra Zeneca, and consumer products company Procter & Gamble have experimented or are currently experimenting with microreactor technologies. However, there is little information on the application, scale, scope, or size of the experimental microreactors (Boswell), and successful applications do not seem to be easily generalized. In 2004, Sigma-Aldrich was reported to have purchased the Cytos Lab System, a microreactor system produced by Cellular Process Chemistry Systems that sells for $70,000 to $200,000 depending on the size, for about $187,000 (Microreactors eyed for industrial use 2004). The Cytos Lab System is reported to be capable of operating from milligram to low tonnage production annually.

Because microreactors are not expected to become widely used in industry for at least another ten years, it is difficult to assess the overall size of the microreactor market at this time. It is estimated that 30% of fine chemicals and drugs currently in production could be produced more efficiently using microreactors. Once the challenges facing microreactor implementation have been addressed, one-fifth of chemical producers are expected to use microreactors in their processes. Currently, research and development departments and highly specialized orders define the microreactor market (Boswell).

The proposed software product, a model predictive controller for stochastic processes for use with microreactors, seeks to overcome challenges with controlling and optimizing microreactors. Since microreactors are still in their early development, there are currently very few customers in need of such a controller. However, online control for microreactors is necessary for the practical implementation of microreactor systems in industry. Therefore, controllers such as the proposed product have great potential because they will have an immediate market as soon as microreactor technologies gain widespread acceptance in industry.

5.2 Profitability Analysis

To determine the profitability and price of a model predictive controller for a μTAS, the viability of selling such a controller to a start-up company producing cyclohexane from the hydrogenation of cyclohexene was explored. Prices of the chemicals involved in the cyclohexene reaction network are given in Table 3.

Table 3 gives the prices of the chemical species used in the control simulations.

Species	Price	Quantity	Description
Cyclohexene	$50	1L	125431-1L on Sigma-Aldrich
Benzene	$60	1L	401765-1L on Sigma-Aldrich
Hydrogen	$165	56L	295396-56L on Sigma-Aldrich
Cyclohexane	$65	1L	227048-1L on Sigma-Aldrich

The bare module costs of the equipment for a hypothetical microreactor start-up company are summarized in Table 4. The price of the Cytos Lab System was used as a general estimate for a microreactor system. The price of a properly outfitted computer was estimated from Dell. The prices of the fume hood, vacuum system, gas chromatograph and catalysts were taken from online vendors. The price of the storage tanks, which were designed to hold up to a month's worth of reactants and products, and the bare model factors were estimated using the metrics in *Product and Process Design Principles: Synthesis, Analysis and Evaluation* (Seider 2010).

Table 4 summarizes the equipment costs for a microreactor start-up in Philadelphia, PA

Equipment Description	Purchase Cost	Bare Module Factor	Bare Module Cost
Microreactor System	$187,000	3.05	$570,350
Computer	$2,000	1.40	$2,800
Fume Hood	$2,000	2.10	$4,200
Vacuum System	$15,000	3.30	$49,500
Storage Tanks	$28,000	4.16	$116,480
Gas Chromatograph	$3,200	2.72	$8,714
Pt (per g powder, 99.99% pure)	$1,024	1.27	$1,299

Several general assumptions were made in this analysis. These include a production life of 15 years with one year each for both design and construction, complete payment of the total permanent investment (TPI) within the first year, and 330 operating days of the plant per year. The plant was constructed to operate at 50% of its production capacity in its first year, reaching operation at 90% of its design capacity in two years. Considering that it is constructed in Philadelphia, PA, USA in 2010, a site factor of 1.10 and income tax rate of 40% were applied. Three plant operators, each with an eight hour workday, were paid $40 per operator per hour. A 3% adjustment for inflation was used for all recurring costs and revenues. The electricity demand was estimated to be 3 kWh per liter of cyclohexane at a price of $0.06 per kWh.

The cost summary calculated by the Profitability Spreadsheet version 3.0 provided in *Product and Process Design Principles* is shown in Figure 24. The total variable costs were $62,800; the total fixed costs were $578,000; and the total capital investment was just over $2MM.

The cash flow summary is shown in Table 5. The cash flow in 2012, the first year of operation, is $113,000 and the cash flow in 2020, ten years after the start of the project, is $517,400. An investor would break even in the year 2020, and the net present value (NPV) of the project in the year 2026 is $576,500. The sensitivity analysis, which displays the investor's rate of return (IRR) for 50% variation in the variable costs and the price of cyclohexane, is shown in Table 6. The IRR was much more sensitive to changes in the product price than in variable costs. For example, with an IRR of 20.49% for the specifications given above, decreasing the variable costs by 50% would only increase the IRR to 21.28%, and increasing the variable costs by 50% would only decrease the IRR to 19.67%. On the other hand, a decrease of 50% in the price of cyclohexane gives a negative IRR and an increase of 50% gives an IRR of 36.17%. Volatility in the price of cyclohexane therefore has a greater impact on the profitability of the start-up company.

If the model predictive control software were bought by the start-up at $18,000, an IRR of 20% would be achieved by the start-up, and the NPV of the project would drop $43,000 to $533,400 assuming a bare module factor of 1.4 for the software.

Variable Cost Summary

Variable Costs at 100% Capacity:

General Expenses

Selling / Transfer Expenses:	$	43,875
Direct Research:	$	70,200
Allocated Research:	$	7,313
Administrative Expense:	$	29,250
Management Incentive Compensation:	$	18,281
Total General Expenses	$	168,919

Raw Materials	$54.996429 per L of µ-TAS Effluent	$1,237,420
Byproducts	$59.892857 per L of µ-TAS Effluent	($1,347,589)
Utilities	$0.180000 per L of µ-TAS Effluent	$4,050

Total Variable Costs	**$**	**62,799**

Fixed Cost Summary

Operations

Direct Wages and Benefits	$	249,600
Direct Salaries and Benefits	$	37,440
Operating Supplies and Services	$	14,976
Technical Assistance to Manufacturing	$	-
Control Laboratory	$	-
Total Operations	**$**	**302,016**

Maintenance

Wages and Benefits	$	69,809
Salaries and Benefits	$	17,452
Materials and Services	$	69,809
Maintenance Overhead	$	3,490
Total Maintenance	**$**	**160,562**

Operating Overhead

General Plant Overhead:	$	26,575
Mechanical Department Services:	$	8,983
Employee Relations Department:	$	22,084
Business Services:	$	27,698
Total Operating Overhead	**$**	**85,341**

Property Taxes and Insurance

Property Taxes and Insurance:	$	31,026

Other Annual Expenses

Rental Fees (Office and Laboratory Space):	$	-
Licensing Fees:	$	-
Miscellaneous:	$	-
Total Other Annual Expenses	**$**	-

Total Fixed Costs	**$**	**578,945**

Investment Summary

Bare Module Costs			
Fabricated Equipment	$	570,350	
Process Machinery	$	53,700	
Spares	$	-	
Storage	$	558,300	
Other Equipment	$	8,714	
Catalysts	$	1,299	
Computers, Software, Etc.	$	2,800	
Total Bare Module Costs:			$ 1,195,163
Direct Permanent Investment			
Cost of Site Preparations:	$	59,758	
Cost of Service Facilities:	$	59,758	
Allocated Costs for utility plants and related facilities:	$	-	
Direct Permanent Investment			$ 1,314,679
Total Depreciable Capital			
Cost of Contingencies & Contractor Fees	$	236,642	
Total Depreciable Capital			$ 1,551,322
Total Permanent Investment			
Cost of Land:	$	31,026	
Cost of Royalties:	$	-	
Cost of Plant Start-Up:	$	155,132	
Total Permanent Investment - Unadjusted			$ 1,737,480
Site Factor			1.10
Total Permanent Investment			$ 1,911,228

Working Capital

	2011	2012	2013
Accounts Receivable	$ 54,092	$ 27,046	$ 27,046
Cash Reserves	$ 21,563	$ 10,781	$ 10,781
Accounts Payable	$ (45,917)	$ (22,959)	$ (22,959)
µ-TAS Effluent Inventory	$ 50,486	$ 25,243	$ 25,243
Raw Materials	$ 3,051	$ 1,526	$ 1,526
Total	**$ 83,275**	**$ 41,638**	**$ 41,638**
Present Value at 15%	*$ 72,413*	*$ 31,484*	*$ 27,377*

Total Capital Investment $ 2,042,503

Figure 24 shows the cost summary for the start-up company.

Table 5 shows the cash flow summary for the start-up company

Year	Percentage of Design Capacity	Product Unit Price	Sales	Capital Costs	Working Capital	Var Costs	Fixed Costs	Depreciation	Depletion Allowance	Taxible Income	Taxes	Net Earnings	Cash Flow	Cumulative Net Present Value at 15%
2010	0%		-	-	-	-	-	-	-	-	-	-	-	-
2011	0%		-	(1,911,200)	(83,300)	-	-	-	-	-	-	-	(1,994,500)	(1,734,400)
2012	45%	$65.00	658,100	-	(41,600)	(28,300)	(578,900)	(310,300)	-	(259,300)	103,700	(155,600)	113,000	(1,648,900)
2013	68%	$66.95	1,016,800	-	(41,600)	(43,700)	(596,300)	(496,400)	-	(119,600)	47,800	(71,800)	383,000	(1,397,000)
2014	90%	$68.96	1,396,400	-	-	(60,000)	(614,200)	(297,900)	-	424,400	(169,800)	254,600	552,500	(1,081,200)
2015	90%	$71.03	1,438,300	-	-	(61,800)	(632,600)	(178,700)	-	565,200	(226,100)	339,100	517,800	(823,700)
2016	90%	$73.16	1,481,500	-	-	(63,600)	(651,600)	(178,700)	-	587,500	(235,000)	352,500	531,200	(594,000)
2017	90%	$75.35	1,525,900	-	-	(65,500)	(671,200)	(89,400)	-	699,900	(279,900)	419,900	509,300	(402,600)
2018	90%	$77.61	1,571,700	-	-	(67,500)	(691,300)	-	-	812,900	(325,200)	487,700	487,700	(243,100)
2019	90%	$79.94	1,618,800	-	-	(69,500)	(712,000)	-	-	837,300	(334,900)	502,400	502,400	(100,300)
2020	90%	$82.34	1,667,400	-	-	(71,600)	(733,400)	-	-	862,400	(345,000)	517,400	517,400	27,600
2021	90%	$84.81	1,717,400	-	-	(73,700)	(755,400)	-	-	888,300	(355,300)	533,000	533,000	142,100
2022	90%	$87.35	1,768,900	-	-	(76,000)	(778,100)	-	-	914,900	(366,000)	549,000	549,000	244,700
2023	90%	$89.98	1,822,000	-	-	(78,200)	(801,400)	-	-	942,400	(376,900)	565,400	565,400	336,600
2024	90%	$92.67	1,876,700	-	-	(80,600)	(825,400)	-	-	970,600	(388,300)	582,400	582,400	418,900
2025	90%	$95.45	1,933,000	-	-	(83,000)	(850,200)	-	-	999,800	(399,900)	599,900	599,900	492,600
2026	90%	$98.32	1,990,900	-	166,600	(85,500)	(875,700)	-	-	1,029,700	(411,900)	617,800	784,400	576,500

Table 6 shows the results of a sensitivity analysis

		Variable Costs										
		$31,400	$37,679	$43,959	$50,239	$56,519	***$62,799***	$69,079	$75,359	$81,639	$87,919	$94,199
Product Price	$32.50	Negative IRR	Negative IRR	Negative IRR	Negative IRR	Negative IRR	Negative IRR	Negative IRR	Negative IRR	Negative IRR	Negative IRR	Negative IRR
	$39.00	2.22%	1.90%	1.58%	1.25%	0.91%	0.57%	0.22%	-0.14%	-0.50%	-0.88%	-1.26%
	$45.50	8.44%	8.20%	7.97%	7.73%	7.48%	7.24%	6.99%	6.74%	6.49%	6.23%	5.98%
	$52.00	13.33%	13.13%	12.94%	12.74%	12.54%	12.34%	12.14%	11.93%	11.73%	11.52%	11.31%
	$58.50	17.53%	17.35%	17.18%	17.00%	16.83%	16.65%	16.47%	16.30%	16.12%	15.94%	15.76%
	$65.00	21.28%	21.13%	20.97%	20.81%	20.65%	20.49%	20.33%	20.16%	20.00%	19.84%	19.67%
	$71.50	24.74%	24.59%	24.45%	24.30%	24.15%	24.00%	23.85%	23.70%	23.55%	23.40%	23.25%
	$78.00	27.98%	27.84%	27.70%	27.56%	27.42%	27.28%	27.14%	26.99%	26.85%	26.71%	26.57%
	$84.50	31.05%	30.91%	30.78%	30.65%	30.51%	30.38%	30.24%	30.11%	29.97%	29.84%	29.70%
	$91.00	33.98%	33.85%	33.72%	33.59%	33.46%	33.33%	33.20%	33.07%	32.94%	32.81%	32.68%
	$97.50	36.80%	36.67%	36.55%	36.42%	36.30%	36.17%	36.05%	35.92%	35.80%	35.67%	35.54%

6. Conclusions

In this report, the production methods and economics of a μTAS integrating model-based control in its microreactors were studied for a reaction network consisting of the hydrogenation and dehydrogenation of cyclohexene. Given the current technology readily available for industrial applications, one of the most cost effective manufacturing process for microreactors would implement anisotropic wet chemical etching for channel fabrication, diffusion bonding followed by microlamination for creating microarrays, and modified anodic oxidation for coating the channels with Sn / Pt(111) alloy catalyst.

The model predictive controller successfully achieved its goals and was found to be highly resistant to the inherent stochasticity of the small-scale processes like those run in microreactors. At volumes of approximately 10^{-20} L, the number of particles was small enough to warrant stochastic control. The controller adjusted the reactor temperature to obtain various effluent stream compositions and regularly reached steady state within 20-30 seconds. The tanks-in-a-series approximation was used to emulate a PFR. Greater production of cyclohexane was observed with increasing number of CSTRs in series. In future studies, the effects of varying the temperature in each of the CSTRs in series should be investigated. Higher quality and/or more valuable effluent streams may be possible with such a control scheme. Further, varying an inert flow rate would also improve control of the effluent stream but may not be profitable.

The market for microreactors is still developing. In ten years, it is projected that 20% of chemical companies will make use of microreactors. Having a robust controller will be necessary for the optimal operation of microreactors on an industrial scale. Through a profitability analysis for a start-up microreactor company based in Philadelphia, PA, USA, a price of $18,000 per license was calculated for the software-based controller in order to achieve a 20% IRR and a break-even point in 2020. Depending on the development of the microreactor industry and the emergence of competitors, this price may need to be reevaluated.

This study is only a preliminary attempt at assessing the functionality and profitability of a software-based controller for stochastic processes. Given the anticipated expansion of microreactor technologies, the proposed product has strong potential to be profitable in the coming years.

7 Acknowledgements

The authors would like to express their gratitude for the invaluable advice provided by Professor Leonard A. Fabiano, Dr. Warren Seider, and Dr. Talid R. Sinno. Professor Fabiano provided the group with general guidance regarding the writing and timeline of the report. Dr. Seider provided assistance in implementing effective control strategies and taught the fundamental skills required to complete a successful product design project through our design course last fall. Dr. Sinno explained the details of the kinetic Monte Carlo method and shaped the strategy that was used to tackle the control and display issues. Additionally, the design consultants provided useful suggestions and advice from an industrial perspective.

8 Bibliography

ACS Publications. *C&EN: Microreactors eyed for industrial use*. Web. 10 Apr. 2010. <http://pubs.acs.org/cen/news/8226/8226earlysci2.html>.

ACS Publications. *C&EN: Microreactors for the chemical masses.* Web. 10 Apr. 2010. <http://pubs.acs.org/cen/news/8248/8248earlybus.html>.

Boswell, C. Microreactors Gain Popularity Among Producers. *ICIS Chemical Business*. [Online] Apr 30, 2009. http://www.icis.com/Articles/2009/05/04/9211877/microreactors-gain-popularity-among-producers.html (accessed Apr 15-16, 2010).

Chen, D., Moljord, K., Fuglerud, T., and Holmen, A., *Microporous and Mesoporous Materials* **29** (1999), p. 191-203

Davis, S.M. and Somoriai, G.A. *J. Catal.* **65** (1980), p. 78.

Ehrfeld, W. , Hessel, V., and Lowe, L. Microreactors: New Technology for Modern Chemistry, Wiley–VCH, Weinheim, Germany (2000) p. 2-29.

Henn, F.C., Diaz, A.L., Bussell, M.E., Hugenschmidt, M.B., Domagala, M.E., and Campbell, C.T. *J. Phys. Chem.* **96** (1992), p. 5965.

Hessel, V., Löwe, H., Müller, A., and Kolb, G., Chemical Micro Process Engineering: Processing and Plants, Wiley–VCH, Weinheim, Germany (2006) p. 324, 385-400

Incropera, F. P., DeWitt, D. P., Bergman, T. L., and Lavine, A. S., Fundamentals of Heat and Mass Transfer, John Wiley & Sons Inc., New York, NY (2007) pp. 524-7.

LabX. Fume Hoods. http://www.labx.com/v2/newad.cfm?catid=9 (accessed Apr 20, 2010).

Li, Y.-(guang), Chang, X., and Zeng, Z., *Ind. Eng. Chem. Res.* **31** (1992) p. 187-92

Nassar, R., Hu, J., Palmer, J., and Dai, W., *Catal. Today* **120** (2007) p. 121-4

Ouyang, X. and Besser, R.S. *Catal. Today* **84** (2003), p. 33.

Pacheco, M., Sira, J., and Kopasz, J., *Applied Catal. A*, **250** (2003) p. 161-75

Rase, H. F., Handbook of Commercial Catalysts : Hetergeneous Catalysts, CRC Press, Washington, D.C. (2000) p. 105-15

Rawlings, J. B. and Ekerdt, J. G., Chemical Analysis and Design Fundamentals, Nob Hill Publishing, Madison, WI (2002) pp. 220-3

Sci-bay. Gow-Mac Series 580 Gas Chromatograph. http://www.sci-bay.com/catalog.asp?prodid=356857&showprevnext=1 (accessed Apr 23, 2010).

Segal, E., Madon, R.J., and Boudart, M.J. *J. Catal.* **52** (1978), p. 45.

Seider, W. D., Seader, J.D., Lewin, D.R., Widagdo, S. Product and Process Deisgn Principles: Synthesis, Analysis and Evaluation, 3rd ed.; Wiley: Hoboken, NJ, 2009.

Sigma-Aldrich. Platinum catalyst pricing. http://www.sigmaaldrich.com/catalog/Lookup.do?N5=All&N3=mode%2Bmatchall&N4=platinum&D7=0&D10=&N25=0&N1=S_ID&ST=RS&F=PR (accessed Apr 19, 2010).

Solaronix. Pt coating service. http://www.solaronix.com/services/ptcoating/ (accessed Apr 19, 2010).

Su, K., Kung, K.Y., Lahtinen, J., Shen, Y.R. and Somorjai, G.A. *J. Mol. Catal. A: Chem.* **141** (1999), p. 9.

Thompson, A and Plimpton, S. "SPPARKS Users Manual." *Sandia National Laboratories*. http://www.sandia.gov/~sjplimp/spparks/doc/Manual.html (accessed Apr 16, 2010).

Voloshin, Y., Halder, R., and Lawal, A., *Catal. Today* **125** (2007), p. 40-7.

Voorhoeve, R. J. H. , Remeika, J. P. , Freeland, P. E. , Matthias, P. T. Rare-earth oxides of manganese and cobalt rival platinum for the treatment of carbon monoxide in auto exhaust. Science 177, 353 (1972).

Watts, P. and Wiles, C., *Chem. Commun.* **1** (2006), p. 443-67

Xu, C. and Koel, B.E. *Surf. Sci.* **304** (1994), p. 249.

Zindarsic-Plazl, P. "Steroid Extraction in a Microchannel System - Mathematical Modelling and Experiments." *Lab Chip* 7 (2007): 883-89.

Zumdahl, S.S. Chemical Principles, 5th ed.; Houghton Mifflin: Boston, MA, 2007.

Appendix A. Setting Up a Problem in SPPARKS

A.1 Input File Structure

A SPPARKS input file consists of three sections. The first section contains commands used to initialize a simulation. These commands include choice of application and choice of solving method. The second section includes commands for various settings and commands specifying simulation parameters. The third section consists of a command to perform the simulation. The second and third sections can be repeated as necessary in order to change settings and/or simulation parameters during the course of a simulation.

The required commands used to perform the simulations presented are explained in the following sections. Some commands are optional and only necessary when a value different from the default is needed. Default values for optional commands can be found in the documentation for SPPARKS. Additional information about using SPPARKS can also be found in the documentation.

Note that SPPARKS accepts values in scientific notation. For example, a value of 1.0×10^{3} would be entered as `1.0e3`, and a value of 1.0×10^{-3} would be entered as `1.0e-3` in SPPARKS.

A.2 `seed`

Each input file begins with the `seed` command. The value set by this command is used as a seed by a master random number generator to initialize auxiliary random number generators that generate random numbers for all operations requiring random numbers. The command is of the form

```
seed Nvalue
```

in which `Nvalue`, which must be a positive integer, is the value of the seed. For example, a seed value of 459 would be set as shown below.

```
seed 459
```

Because SPPARKS is a stochastic simulator, this command must appear in every input file. For a given system, performing simulations with different seed values will give varied results.

A.3 `app_style`

The `seed` command is followed by the choice of application for the simulation, specified by the `app_style` command. The command is of the form

```
app_style style args
```

in which `style` is the name of the application chosen for the simulation and `args` includes zero or more arguments specific to the application chosen. In this case, the `app_style chemistry` application for a system of coupled chemical reactions, which takes no additional arguments, is chosen. Thus, the command takes the following form.

```
app_style chemistry
```

A.4 `solve_style, sweep`

A choice of solution method follows the choice of application. The `app_style chemistry` application is not an on-lattice application involving defined lattice sites and must be solved with a KMC algorithm. Because the `sweep` command instructs SPPARKS to use a rKMC algorithm only suitable for on-lattice applications, a KMC solver must be chosen for the simulation. The command is of the form

```
solve_style style args keyword value ...
```

in which `style` is the name of the chosen solver. `args`, `keyword`, and `value` are only applicable to the `group` solver and will not be elaborated here, as explained below. Three solvers are available: `solve_style linear`, `solve_style tree`, and `solve_style group`. For a simulation with few events from which to choose, the `solve_style linear` solver, which chooses events from a list of events, is appropriate and is chosen. The command thus takes the following form.

```
solve_style linear
```

The `solve_style tree` and `solve_style group` solvers are more appropriate for simulations with greater numbers of possible events and/or large numbers of sites. Depending on the complexity of the system, these solvers may give shorter simulation times. As they were unnecessary for the simulations presented, they will not be discussed further. Instructions for using these solvers, with information about the algorithms they employ, can be found in the documentation for SPPARKS.

A.5 `volume`

The `volume` command sets the volume of the system in the `app_style chemistry` application. The command is of the form

```
volume V
```

in which `V` is the volume of the system in liters. For example, a volume of 1 μL or 1×10^{-6} L would be entered as shown below.

```
volume 1e-6
```

A.6 `add_species`

Chemical species are added to the system via the `add_species` command. The command is of the form

```
add_species name1 name2 ...
```

in which `name1` and `name2` are names of chemical species. Multiple species may be added in a single command, or species may be added individually in multiple commands. More species may be added in a single command, represented by . . . above. For example, species A, B, and C may be added either in a single command or in a series of commands as shown below.

```
add_species A B C
```

or

```
add_species A
add_species B
add_species C
```

Names may contain any non-whitespace characters. For example, species C_6H_6 may be added as shown below.

```
add_species C6H6
```

A system may contain any number of species.

A.7 `add_reaction`

Chemical reactions are defined with the `add_reaction` command. The command is of the form

```
add_reaction reactant1 reactant2 rate product1 product2 ...
```

in which `reactant1` and `reactant2` are names of reactants, `rate` is the rate constant, and `product1` and `product2` are names of products. A reaction may involve one or two reactants and one or more products. Their names are those specified by the `add_species` command. The number of reactants participating in a reaction determines the unit(s) of the rate constant: s^{-1} for one reactant, or L mol^{-1} s^{-1} or M^{-1} s^{-1} for two reactants. For example, a reaction A + B → C involving the species from above with a rate constant of 1 L mol^{-1} s^{-1} or 1 M^{-1} s^{-1} would be entered as shown below.

```
add_reaction A B 1 C
```

Any number of reactions may be defined for a system.

Reactions involving zero reactants or zero products are allowed and can be utilized to add or remove particles to or from a system in order to simulate a CSTR, for example.

A.8 `count`

The `count` command sets the initial number of particles of a species and is of the form

```
count species N
```

in which `species` is the name of the species and `N` is the initial number of particles of the species. The name is that specified by the `add_species` command. For example, an initial number of 10^6 particles of species A from above would be entered as shown below.

```
count A e6
```

Note that the `count` command does not accept values

Appendix B. Code for Controller and Grapher

(requires compiled SPPARKS and JQuery library from http://jquery.com/)

```
<script type="text/javascript" src="jquery.js"></script>
<script type="text/javascript">
$(document).ready(function(){
     $("a").next().hide();
     $("a").click(function(event){
               $(this).next().toggle("slow");
     });
});
</script>

<? // This page will create an input file and execute it.  Details
     in log.1.

ini_set('display_errors', 1);
ini_set('log_errors', 1);
//ini_set('error_log', dirname(__FILE__) . '/error_log.txt');
error_reporting(E_ALL);
     $avo = 6.022e23;
     $ca0 = 1;
if(!isset($_GET['numSec'])){ ?>
     <form method='GET'>
               tMin: <input type="text" name="tMin" value="200"  /><br
               />
               temp: <input type="text" name="temp" value="400"  /><br
               />
               tMax: <input type="text" name="tMax" value="600"  /><br
               />
               vol (x,y,z in um): <input type="text" name="vol"
               value=".01,.01,.1"  /><br />
               reactors: <input type="text" name="reactors" value="5"
               /><br />
               timesteps: <input type="text" name="numSec" value="50"
               /><br />
               timestep length: <input type="text" name="run"
               value="1"  /><br />
               rxn rate multiplier: <input type="text" name="rxnmult"
               value="1"  /><br />
               feed rate (mols A,E per timestep): <input type="text"
               name="feed" value="3000,3000"  /><br />
               initial charge (mols A,E): <input type="text"
               name="initialcharge" value="6022,6022"  /><br />
               max y axis: <input type="text" name="scale"
               value="10000"  /><br />
               controller (1 or 0): <input type="text"
               name="controller" value="1"  /><br />

          <input type="submit" value="Run It!" />
     </form>
<? }
else{
```

```
    echo "<xmp>";
    print_r($_GET);
    echo "</xmp><br />";
    $pastMovements = array(0,1,2);
    $temperatureVary = 100;

    // DEFAULTS //
    if(isset($_GET['tMin'])){ $tMin = $_GET['tMin']; } else{ $tMin =
        200; }
    if(isset($_GET['temp'])){ $temperature = $_GET['temp']; }
        else{ $temperature = 400; }
    if(isset($_GET['tMax'])){ $tMax = $_GET['tMax']; } else{ $tMax =
        600; }
    if(isset($_GET['vol'])){ $vol = $_GET['vol']; } else{ $vol =
        ".01,.01,.1"; }
    if(isset($_GET['reactors'])){ $reactors = $_GET['reactors']; }
        else{ $reactors = 5; }
    if(isset($_GET['numSec'])){ $numSec = $_GET['numSec']; }
        else{ $numSec = 50; }
   if(isset($_GET['run'])){ $run = $_GET['run']; } else{ $run = 1; }
    if(isset($_GET['rxnmult'])){ $rxnmult = $_GET['rxnmult']; }
        else{ $rxnmult = 1; }
    if(isset($_GET['feed'])){ $feed = $_GET['feed']; } else{ $feed =
        "3000,3000"; }
    if(isset($_GET['initialcharge'])){ $initialcharge =
        $_GET['initialcharge']; } else{ $initialcharge =
        "6022,6022"; }
    if(isset($_GET['scale'])){ $scale = $_GET['scale']; }
        else{ $scale = "10000"; }
    if(isset($_GET['controller'])){ $controller =
        $_GET['controller']; } else{ $controller = 1; }

?>
    <form method='GET'>
            temp: <input type="text" name="temp"
            value="<?=$temperature?>" /> tMin: <input type="text"
            name="tMin" value="<?=$tMin?>"  /> tMax: <input
            type="text" name="tMax" value="<?=$tMax?>"  /><br />
            reactors: <input type="text" name="reactors"
            value="<?=$reactors?>" /> vol (x,y,z in um): <input
            type="text" name="vol" value="<?=$vol?>"  /><br />
            timestep length: <input type="text" name="run"
            value="<?=$run?>" /> timesteps: <input type="text"
            name="numSec" value="<?=$numSec?>"  /><br />
            rxn rate multiplier: <input type="text" name="rxnmult"
            value="<?=$rxnmult?>" /><br />
            initial charge (mols A,E): <input type="text"
            name="initialcharge" value="<?=$initialcharge?>"  /><br
            />
            feed rate (mols A,E per timestep): <input type="text"
            name="feed" value="<?=$feed?>" /><br />
            max y-axis: <input type="text" name="scale"
            value="<?=$scale?>" /><br />
            controller (1 or 0): <input type="text"
```

```
            name="controller" value="<?=$controller?>" />

        <input type="submit" value="Run It!" />
    </form>
    <a href="#">Toggle the details.</a><div>
<?php
    $tempInit = $temperature;
    $comma1 = strpos($vol,",");
    $comma2 = strpos($vol,",",$comma1+1);
    $vol = substr($vol,0,$comma1)*substr($vol,$comma1+1,$comma2-
        $comma1-1)*substr($vol,$comma2+1)*pow(10,-15);
    $feedA = substr($feed,0,strpos($feed,","));
    $feedE = substr($feed,strpos($feed,",")+1);
    $initA = substr($initialcharge,0,strpos($initialcharge,","));
    $initE = substr($initialcharge,strpos($initialcharge,",")+1);

    if($feedA+$feedE > $initA+$initE){ echo "this may cause errors
        because the flow rate is higher than the reactor size.  try
        reducing the feed rate and decreasing the timestep in order
        to account for the discrepencies"; }

    // SET DATA LOCATIONS //
    $timer = time();
    $numSeconds = $numSec; //20
    $counts = array(array(array())); //
        counts[reactor#][time][component]
    $time = array();
//  $temperatures = array();
    $mw = array(82,2,84,78,40);
    $r1 = 0;
    $r2 = 0;
    $wait = 0;

    // INITIAL CONDITIONS //
    for($i = 0; $i < $reactors; $i++){
            $counts[$i][0] = array('time'=>0, "a"=>$initA, "b"=>0,
            "c"=>0, "d"=>0, "e"=>$initE, 'temperature' =>
            $temperature);
    }
    for($t=0; $t<$numSec; $t++){
            for($r=0; $r<$reactors; $r++){
                    $random = rand();
                    $input = "./logs/$timer-input1-$random.txt";
                    $output = "./logs/$timer-log-$random.txt";

                    // SET TEMPERATURE / RUN RXN //

                    initialize($counts,$r,$temperature,$tMin,$tMa
                x,$vol,$feed,$mw,$t,$numSeconds,$initialcharge,$wa
                it,$controller,$pastMovements,$temperatureVary,$re
                actors);

                    makeInput($vol,$counts,$r,$r1,$r2,$input,$out
                put,$t,$rxnmult,$run,$reactors);
```

```
                    exec("./spk_mac < $input");
                    // GATHER DATA AND PUT IT IN ARRAYS 'A' AND
                'B' //

                    getData($counts,$r,$t,$output,$mw,$ca0,$vol,$
                avo,$temperature);
                    echo "<hr />";
            }
}
echo "</div><br /><br />";


// OUTPUT THE DATA //  counts[reactor#][time][component]
$reactorPlot = count($counts)-1/*0*/;
$chd = "$initA,";
foreach($counts[$reactorPlot] as
    $tempval){ $chd.=$tempval['a'].","; }
$chd = substr($chd, 0, -1);
$chd .= "|0,";
foreach($counts[$reactorPlot] as
    $tempval){ $chd.=$tempval['b'].","; }
$chd = substr($chd, 0, -1);
$chd .= "|0,";
foreach($counts[$reactorPlot] as
    $tempval){ $chd.=$tempval['c'].","; }
$chd = substr($chd, 0, -1);
$chd .= "|0,";
foreach($counts[$reactorPlot] as
    $tempval){ $chd.=$tempval['d'].","; }
$chd = substr($chd, 0, -1);
$chd .= "|$initE,";
foreach($counts[$reactorPlot] as
    $tempval){ $chd.=$tempval['e'].","; }
$chd = substr($chd, 0, -1);
if($controller){
        $chd .= "|$tempInit,";
        foreach($counts[$reactorPlot] as
        $tempval){ $chd.=$tempval['temperature'].","; }
        $chd = substr($chd, 0, -1);
} ?>

<body>
<form action='http://chart.apis.google.com/chart' method='POST'
    id='chartForm' target="_blank">
  <input type="hidden" name="cht" value="lc"  />
  <input type="hidden" name="chs" value="750x400" />
  <input type="hidden" name="chxt" value="x,x,y" /> <!-- name
      the axes -->
  <input type="hidden" name="chxr"
      value="0,0,<?=$numSeconds*$run?>,<?=$numSeconds*$run/10?>
      |2,0,<?=$scale?>,<?=$scale/10?>" />
  <input type="hidden" name="chxl" value="1:|Time (s)" />
  <input type="hidden" name="chf" value="a,s,000000" />
  <input type="hidden" name="chxp" value="1,50|3,50" />
```

```
      <input type="hidden" name="chco"
           value="FF0000,0000FF,00FF00,666666,000000,8B3A62" /> <!--
           color of lines -->
      <input type="hidden" name="chds" value="0,<?=$scale?>" /> <!--
           height of graph -->
      <input type="hidden" name="chg" value="10,10" /> <!-- spacing
           of the dotted lines -->
      <input type="hidden" name="chdl" value="C6H10 (cyclohexene,
           82)|H2 (hydrogen, 2)|C6H12 (cyclohexane, 84)|C6H6
           (benzene, 78)|Inert (argon, 40)<?php
           if($controller){?>|Temperature (K)<? } ?>" /> <!-- legend
           text -->
      <input type="hidden" name="chtt" value="<?=$reactors?>
           Reactors, Vol = <?=$vol?>L, Final Temperature =
           <?=round($temperature)?>K, Rxn 1 Rate = <?=$rxnmult?>|
           Feed = <?=$feed?> molecules, Initial =
           <?=$initialcharge?> Timestep = <?=$run?>" /> <!-- title
           text -->
      <input type="hidden" name="chd" value="t:<?=$chd?>"/> <!--
           data -->
      <input type="submit" value="Graph It!" />
    </form>

    <?
    echo "<a href=\"#\">Toggle the logs.</a><div><br /> Logs are in
         /logs/$random<br />
    </body><xmp>";
    $i=$reactors-1;
    foreach($counts[$i] as $times){
             echo
             $times['time'].",".$times['a'].",".$times['b'].",".$tim
             es['c'].",".$times['d'].",".$times['e'].",".$times['tem
             perature']."\r\n";
    }
    echo "</xmp><hr /><xmp>";
echo "</xmp></div></body>";
}



// INITIALIZE ALL VARIABLES //
function
    initialize($counts,$r,$temperature,$tMin,$tMax,$vol,$feed,$mw,$t
    ,$numSeconds,$initialcharge,$wait,$controller,$pastMovements,$te
    mperatureVary,$reactors){
    global
         $time,$counts,$r1,$r2,$temperature,$vol,$avo,$wait,$pastMov
         ements,$temperatureVary; //make these accessible outside
         this function //
    // THESE DON'T CHANGE //
    $avo = 6.022e23;
    $boltz = 1.381e-23;
    $R = 8.314; // J/molK
    $n1 = 1;
```

```
    $n2 = 1;
    $ca0 = 1;           //.03447 = 400K, 11604 K per eV

    $E1 = 21700; // J/mol
    $E2 = 1920; // J/mol
    $k1 = 218; // L/min
    $k2 = 0.160; // L/mol

    if($controller)    $temperature =
        chooseTemp($vol,$tMin,$tMax,$t,$numSeconds,$temperature,$co
        unts,$r,$R,$E1,$E2,$k1,$k2,$wait,$pastMovements,$temperatur
        eVary,$reactors);
    else $temperature = $temperature;
//print_r($counts);
//echo "<br />";

    $pressure = $counts[$r][count($counts[$r])-1];
    $pressure =
        $pressure['a']+$pressure['b']+$pressure['c']+$pressure['d']
        +$pressure['e'];
//  echo "num mols = $pressure";
    $pressure = $pressure / $avo * 0.08206 * $temperature / $vol;
    echo "Pressure = ".round($pressure,1)." atm.";

    $r1 = $k1*exp(-$E1/($R*$temperature));
    $r2 = $k2*exp(-$E2/($R*$temperature));
//  echo "r1 = $r1, r2 = $r2<br />";

    $feedA = substr($feed,0,strpos($feed,","));
    $feedE = substr($feed,strpos($feed,",")+1);
    $initA = substr($initialcharge,0,strpos($initialcharge,","));
    $initE = substr($initialcharge,strpos($initialcharge,",")+1);
//  echo "$initA.$initE";

    if($r==0 && $t==0){     // FEED STREAM PLUS INITIAL CHARGE
            $push = array("a"=>$feedA, "b"=>0, "c"=>0,
            "d"=>0,'e'=>$feedE);
            $tempy = array("a"=>$initA/$reactors, "b"=>0, "c"=>0,
            "d"=>0,'e'=>$initE/$reactors); //EDITS
    }
    elseif($r == 0){   // FEED STREAM FLOW RATE
            $push = array("a"=>$feedA, "b"=>0, "c"=>0,
            "d"=>0,'e'=>$feedE);
            $tempy = $counts[$r][$t-1];
    }
    elseif($t == 0){   // INITIAL CHARGE
            $push = $counts[$r-1][$t]['push'];
            $tempy = array("a"=>$initA/$reactors, "b"=>0, "c"=>0,
            "d"=>0,'e'=>$initE/$reactors); //EDITS
    }
    else{                   // QUANTITY PUSHED TO ARRAY
//    echo "amount pushed to this array";
//    print_r($counts[$r-1][$t]);
            $push = $counts[$r-1][$t]['push'];
```

```
            $tempy = $counts[$r][$t-1];
    }
    $particlesInitial = $initA + $initE;
    $particlesPushed =
        $push['a']+$push['b']+$push['c']+$push['d']+$push['e'];

    if($particlesInitial == 0){ $ratio = 1; echo "ERROR!"; }
    else{ $ratio = $particlesPushed/$particlesInitial; }

    $counts[$r][$t] = array('a'=>round($tempy['a']*(1-
        $ratio)+$push['a']), 'b'=>round($tempy['b']*(1-
        $ratio)+$push['b']), 'c'=>round($tempy['c']*(1-
        $ratio)+$push['c']), 'd'=>round($tempy['d']*(1-
        $ratio)+$push['d']), 'e'=>round($tempy['e']*(1-
        $ratio)+$push['e']), 'push'=>
        array('a'=>round($tempy['a']*$ratio),
        'b'=>round($tempy['b']*$ratio),
        'c'=>round($tempy['c']*$ratio),
        'd'=>round($tempy['d']*$ratio),
        'e'=>round($tempy['e']*$ratio)));


}

// CONTROLLER //
function
    chooseTemp($vol,$tMin,$tMax,$t,$numSeconds,$temperature,$counts,
    $r,$R,$E1,$E2,$k1,$k2,$wait,$pastMovements,$temperatureVary,$rea
    ctors){
    global $temperature,$wait,$pastMovements,$temperatureVary;
    $numToCount = 5; // will use this many closest and one step away
        further
    $tolerance = .1; // how close do the numbers need to be?
    $percentDone = $t / $numSeconds;

    $recents = array_slice($counts[$r], count($counts[$r])-
        2*$numToCount);
    $recentShort = array_slice($recents, count($recents)-
        $numToCount);
    $longAverage = 0;
    foreach($recents as $temp){
            $longAverage+= $temp['a'];
    }
    $longAverage /= 2*$numToCount;
    $shortAverage = 0;
    foreach($recentShort as $temp){
            $shortAverage+= $temp['a'];
    }
    $shortAverage /= $numToCount;
//  echo "avg1 = $longAverage, avg2 = $shortAverage";
    if($wait >= 5 && $longAverage!=0 && $longAverage*(1+$tolerance)
        > $shortAverage && $longAverage/(1+$tolerance) <
        $shortAverage){
```

```
            if($pastMovements[count($pastMovements)-
            1]==$pastMovements[count($pastMovements)-3]){
                      $temperatureVary /= 2;
                      if($temperatureVary < 1) $temperatureVary=1;
                      echo "gonna vary by $temperatureVary";
            }else { }
            $temperatureVary = 7;

            echo "   <b>STEADY STATE</b> @ t=",$counts[$r][$t-
            1]['time'];
            $timer = time();
            $random = rand();
            $inputHigh = "./logs/$timer-input1-$random-high.txt";
            $outputHigh = "./logs/$timer-log-$random-high.txt";
            $inputLow = "./logs/$timer-input1-$random-low.txt";
            $outputLow = "./logs/$timer-log-$random-low.txt";
            if($temperature+$temperatureVary < $tMax){ $tHigh =
            $temperature+$temperatureVary; } else { $tHigh =
            $tMax; }
            if($temperature-$temperatureVary > $tMin){ $tLow =
            $temperature-$temperatureVary; } else { $tLow = $tMin; }
            $r1high = $k1*exp(-$E1/($R*$tHigh));
            $r2high = $k2*exp(-$E2/($R*$tHigh));
            $r1low = $k1*exp(-$E1/($R*$tLow));
            $r2low = $k2*exp(-$E2/($R*$tLow));
            $countsTemp = $counts[$r][count($counts[$r])-1];
            $rtemp =
            array(0=>array(0=>array('a'=>$countsTemp['a']*100,
            'b'=>$countsTemp['b']*100, 'c'=>$countsTemp['c']*100,
            'd'=>$countsTemp['d']*100, 'e'=>$countsTemp['e']*100)));

                makeInput($vol*100,$rtemp,0,$r1high,$r2high,$inputH
            igh,$outputHigh,0,1,.2,$reactors);

                makeInput($vol*100,$rtemp,0,$r1low,$r2low,$inputLow
            ,$outputLow,0,1,.2,$reactors);

            exec("./spk_mac < $inputHigh");
            exec("./spk_mac < $inputLow");

            $file2High = fopen("./".$outputHigh, 'r') or die("can't
            open file2");
            $dataHigh = fread($file2High,
            filesize("./".$outputHigh));
            fclose($file2High);
            $dataHigh = explode("\n",$dataHigh);
            $tempHigh = preg_split("/[\s]+/", $dataHigh[21]);
//   print_r($temporary);
            $file2Low = fopen("./".$outputLow, 'r') or die("can't
            open file2");
            $dataLow = fread($file2Low, filesize("./".$outputLow));
            fclose($file2Low);
            $dataLow = explode("\n",$dataLow);
            $tempLow = preg_split("/[\s]+/", $dataLow[21]);
```

```
                // 3 = cyclohexene
                // 4 = hydrogen
                // 5 = cyclohexane
                // 6 = benzene


//    $highConversion = $tempHigh[5]/$tempHigh[6];
      //MAXIMIZE BENZ
//    $lowConversion = $tempLow[5]/$tempLow[6];
            //MAXIMIZE BENZ
//    if($highConversion > $lowConversion){ $temperature = $tHigh; }

                $highConversion = $tempHigh[6]/$tempHigh[5];
                    // COMPARING BENZ AND CYCLOHEX
                $lowConversion = $tempLow[6]/$tempLow[5];
                    // COMPARING BENZ AND CYCLOHEX
                if(abs($highConversion-1) < abs($lowConversion-1))
                    { $temperature = $tHigh; }


                else
                                { $temperature = $tLow;  }
                echo ". Move temp to $temperature. ";
                $pastMovements[] = $temperature;
                $wait = 0;
        }
        else{
                if(isset($counts[$r][$t-1]['time'])) $tima =
                $counts[$r][$t-1]['time']; else $tima = 0;
                echo "   <i>NOT STEADY STATE</i> @ t=$tima. Keep temp
                at $temperature.  ";
                $wait++;
        }
        return $temperature;
}


// MAKE THE INPUT FILE // vol = 1.9098395e-11
function
     makeInput($vol,$counts,$r,$r1,$r2,$input,$output,$t,$rxnmult,$ru
     n,$reactors){
     $file = fopen($input, 'w') or die("can't open file");
     $random = rand();
     $tempy = array_keys($counts[$r]);
     $timer = $tempy[count($tempy)-1];
     $r1 *= $rxnmult;
     $vol /= $reactors;
//   echo " ",$input," ";
     $text = "
     seed $random
     log $output
     app_style          chemistry
     solve_style        linear
```

```
    add_species         A
    add_species         B
    add_species         C
    add_species         D
    add_species         E
    volume $vol

    count  A     ".$counts[$r][$timer]['a']."
    count  B     ".$counts[$r][$timer]['b']."
    count  C     ".$counts[$r][$timer]['c']."
    count  D     ".$counts[$r][$timer]['d']."
    count  E     ".$counts[$r][$timer]['e']."
    add_reaction 1     A B   $r1   C
    add_reaction 2     A     $r2   D B B
    stats              $run
    run                $run
    ";
    fwrite($file, $text);
    fclose($file);
}



// COLLECT THE DATA FROM THE LOG FILES //
function
    getData($counts,$r,$t,$output,$mw,$ca0,$vol,$avo,$temperature){
    global $counts,$r; //make these accessible outside this function
        //

    $file2 = fopen("./".$output, 'r') or die("can't open file2");
    $data = fread($file2, filesize("./".$output));
    fclose($file2);
    $data = explode("\n",$data);

    $timeSoFar = max($counts[$r]);
    if(isset($timeSoFar['time'])){
            $timeSoFar = $timeSoFar['time']; // time elapsed is the
            largest time in counts[r]
    }
    else{  // this should only happen for reactor 0 which has been
        prefilled with initial counts.
            $timeSoFar2 = max(array_keys($counts[$r]))-1;
            if(isset($counts[$r][$timeSoFar2]['time'])){
                    $timeSoFar  =  $counts[$r][$timeSoFar2]['time'];
            }
            else{
                     $timeSoFar = 0;  // this should only happen
                for reactor 0 time 0
            }
    }
    $temporary = preg_split("/[\s]+/", $data[21]);
    $timeSoFar3 = $timeSoFar + $temporary[1];
```

```
        ///////// ADD STUFF FROM REACTOR ///////
        $counts[$r][$t] = array('time'=>$timeSoFar3, 'a'=>$temporary[3],
            'b'=>$temporary[4], 'c'=>$temporary[5], 'd'=>$temporary[6],
            'e'=>$temporary[7], 'temperature' => $temperature) +
            $counts[$r][$t];

}
?>
```